Scientific Reports

https://doi.org/10.1038/s41598-026-41570-8

Article in Press

Experimental performance comparison of fixed and single-axis subfields in a large-scale outdoor photovoltaic power plant

Received: 1 June 2025

Accepted: 20 February 2026

Published online: 05 March 2026

Cite this article as: Abderraouf B., Lakhdar L.M., Abdelkader B. *et al.* Experimental performance comparison of fixed and single-axis subfields in a large-scale outdoor photovoltaic power plant. *Sci Rep* (2026). https://doi.org/10.1038/s41598-026-41570-8

Bouramdane Abderraouf, Louazene Mohammed Lakhdar, Benmir Abdelkader, Larouci Benyekhlef, Salah K. Elsayed, Abdulrahman Babqi, Daniel Limenew Meheretie & Walid S. E. Abdellatif

Experimental Performance Comparison of Fixed and Single-Axis Subfields in a Large-Scale Outdoor Photovoltaic Power Plant

Bouramdane Abderraouf[1,*], Louazene Mohammed Lakhdar[1], Benmir Abdelkader[1], Larouci Benyekhlef[1,2], Salah K. Elsayed[3], Abdulrahman Babqi[3], Daniel Limenew Meheretie[4,*], Walid S. E. Abdellatif[5]

[1]Laboratory of Electrical Engineering (LAGE), Department of Electrical Engineering, University of kasdi Merbah Ouargla, Ouargla 30000, Algeria
bouramdane.abderraouf@univ-ouargla.dz; Lakhdar.louazene@gmail.com; ge.abenmir@gmail.com;
[2]Department of Electrical Engineering, University Kasdi Merbah Ouargla, Algeria, Smart Grid Development Laboratory, ESGEEO, Oran; Algeria; larouci.benyekhlef@univ-ouargla.dz
[3]Department of Electrical Engineering, College of Engineering, Taif University, Taif 21944, Saudi Arabia; sabdelhamid@tu.edu.sa; ajbabqi@tu.edu.sa
[4]Department of Electrical and Computer Engineering, Faculty of Technology, Debre Markos University, P. BOX 269, Debre Markos, Ethiopia; daniel_limenew@dmu.edu.et
[5]Electrical Department, Faculty of Technology and Education, Suez University, Suez 43527, Egypt; Walid.Abdellatif@suezuniv.edu.eg

*Corresponding author: Bouramdane Abderraouf (e-mail: bouramdane.abderraouf@univ-ouargla.dz); Daniel Limenew Meheretie(e-mail: daniel_limenew@dmu.edu.et)

ABSTRACT: This study analyzes the power production (PP) and energy yield of four 100 kW PV subfields, consisting of monocrystalline and polycrystalline technologies, with fixed and single-axis tracking systems. All subfields are installed at a 30° inclination, close to the region's optimal angle. Actual performance data were recorded every four minutes in OUED-NECHOU, Ghardaïa, over four experimental days in 2016, each representing a different season. The results indicate that single-axis tracking subfields consistently outperformed fixed systems throughout the diurnal cycle by generating more power and enhancing overall performance. However, on May 1st, the fixed mc-Si and pc-Si subfields reached peak outputs of 95.67 kW and 84.06 kW, respectively, surpassing the motorized subfields, which recorded 88.35 kW and 83.01 kW. Conversely, on July 1st, the single-axis tracking systems achieved their highest daily energy generation, with the mc-Si subfield producing 787.94 kWh/day and the pc-Si single-axis system generating 715.17 kWh/day. Further analysis of mean power output augmentation demonstrated that single-axis tracking subfields consistently outperformed their fixed counterparts, which served as the baseline across all experimental days, with the highest gains observed in east-west tracking systems. On July 1st, the mc-Si tracking system achieved a 19.22% increase over the fixed mc-Si subfield, while the pc-Si tracking subfield exceeded its fixed counterpart by a remarkable gain of 21.44%. Moreover, tracking systems exhibited a clear advantage in maximizing solar energy capture, leading to higher energy production. Finally, the impact of weather conditions, including solar irradiance, temperature, wind speed, and relative humidity, on PV subfield power generation was experimentally analyzed.

keywords: Experimental simulation, Fixed PV systems, Optimal inclination angle, Photovoltaic sub-fields, Power production, Single-axis tracking systems, Weather conditions, Performance evaluation, Power output, Power gain, Energy yield.

1. Introduction

Energy production presents a significant challenge for the near future. Currently, fossil fuels remain the primary source of global energy, contributing heavily to greenhouse gas emissions and accelerating climate change. The rapid depletion of these finite resources, due to excessive consumption, emphasizes the need for sustainable alternatives Haddad et al., [1] and Saiah and Stambouli [2]. In this context, the demand for renewable energy sources has become increasingly urgent. Renewable energy, particularly solar, wind, and hydropower, is gaining recognition as a viable solution to meet the rising global energy demand. However, the intermittent nature of these sources necessitates efficient and cost-effective energy storage solutions. Zhang et al., 2024 [3] presented a thorough review of iron-based redox flow batteries (Fe-RFBs), which are becoming a promising solution for large-scale energy storage. Their study examined the historical development, essential performance factors, and recent advancements in Fe-

RFB technology. It emphasized the advantages of Fe-RFBs, including their cost-effectiveness, environmental benefits, and potential to facilitate the integration of renewable energy sources. The findings highlighted that iron-redox flow batteries (Fe-RFBs) have advantages such as a long cycle life and scalability, but they still face challenges. These challenges included mitigating hydrogen evolution, improving electrode stability, and enhancing overall efficiency. To tackle these issues, the authors recommended optimizing electrode materials, developing cost-effective active components, and refining system design to boost performance and commercial viability. These advancements have the potential to significantly improve energy storage capacity, thereby contributing to the stability and sustainability of renewable energy systems.

These advancements could significantly improve energy storage capacity, Promoting the stability and sustainability of renewable energy systems and given the increasing reliance on solar energy, integrating efficient energy storage benefits, particularly in sun-rich regions like Algeria.

With its exceptional year-round sunshine, Algeria is well-positioned for large-scale solar energy deployment (Stambouli et al., 2012) [4]. In recent years, government initiatives have driven significant progress in renewable energy, including establishing of photovoltaic power plants in the Saharan regions to enhance solar capacity. For example, as part of its renewable energy strategy for the Saharan regions, Sonelgaz (The National Gas and Electricity Society) has established photovoltaic power plants in the OUED-NECHOU region of Ghardaïa. These plants, managed by SKTM (Electricity & Renewable Energy Company), have a combined production capacity of approximately 1.1 MW. Ensuring that these photovoltaic modules operate reliably for 20–25 years under field conditions is critical to maintaining profitability (Sharma and Chandel., 2013 [5]. This initiative underscores Algeria’s commitment to clean energy and sustainable development, paving the way towards a greenr and more eco-friendly future Dahmoun et al., 2021 [6]. Understanding the performance of photovoltaic (PV) systems is essential for evaluating the potential of solar energy as a reliable power source. Analyzing the efficiency and operation of these systems provides valuable insights into their maintenance needs and long-term economic viability Dahmoun et al., 2021[6]. PV systems rapidly emerged as a dominant sustainable electricity source, representing a promising alternative to conventional energy sources. Their performance, however, depends largely on the technology used and the system's design. Numerous studies have assessed PV plant performance in various geographic regions, emphasizing how local environmental conditions influence system efficiency. Large-scale photovoltaic public-private partnership (LS-PVPP) projects have been analyzed globally, with findings from some reported in the literature Ascencio-Vasquez et al., 2021 [7]. Bentouba et al., 2021 [8]. For instance, Shiva Kumar and Sudhakar (2015) [9], studied a 10 MWp photovoltaic plant in India, reporting a yield factor (YF) ranging from 1.96 to 5.07 hours per day, an annual performance ratio (PR) of 86.12%, and a capacity factor (CF) of 17.68%, with an annual energy generation of 15,798.192 MWh. Similarly, Touili et al., (2019) [10]. They found that a 100 MWp plant in the MENA region produces an average of 158 GWh annually. In comparison, the same configuration generates 155.8 GWh annually in Almeria, Spain, and 155.4 GWh in Bakersfield, California. Maximizing the performance of photovoltaic (PV) solar panels relies on capturing as much sunlight as possible. Solar tracking systems are a key technology in achieving this, as they enable PV panels to continuously align with the sun's movement. By adjusting along vertical or horizontal axes, these systems optimize electricity production by ensuring that the panels are always positioned to capture maximum sunlight. As noted by Gomez-Uceda et al., (2021) [11]. Photovoltaic plants equipped with sun tracking systems are designed to follow the sun’s trajectory, ensuring that panels remain perpendicular to the solar rays throughout the day, thereby maximizing power generation. Numerous studies have analyzed the efficiency of solar tracking systems compared to fixed installations. George et al., (2015)[12]. Two off-grid PV systems in Italy one fixed and the other equipped with a daily single-axis solar tracker were analyzed. Their results indicated higher power production in the morning and evening with the single-axis tracker, in contrast to the fixed system. This supports the broader consensus in the literature that tracking systems consistently outperform fixed

PV systems in terms of energy generation Nsengiyumva et al., 2018 [13] Chien-Hsing et al., 2022) [14]. Further studies by Zaghba et al., (2018) [15] and Zaghba et al., (2019) [16] demonstrated that solar tracking systems significantly increase energy capture compared to stationary systems. Vaziri Rad et al., (2020) [17] examined various tracking systems across different regions of iran, finding that twin-axis trackers increased energy generation by 32%, while single-axis trackers led to a 23% increase compared to stationary systems. These findings highlight the critical role of tracking technology in enhancing the efficiency and overall performance of photovoltaic power plants. Recent literature documents both significant advances and practical challenges in solar tracking technologies. The comprehensive review by Kumba et al., (2024) [18] summarizes performance gains achievable with modern trackers while also highlighting the trade-offs of increased mechanical complexity, maintenance requirements, and the need for robust control algorithms. Empirical work on alternative mechanical architectures such as the second-order lever single-axis tracker evaluated by Kumba et al., (2022) [19] demonstrates that innovative designs can improve solar capture and reduce actuator demands under real field conditions. Field studies in high-irradiance environments, such as the Manta, Ecuador case study Ponce-Jara et al., (2024) [20], further confirm that well-designed single-axis tracking systems can significantly increase daily and long-term energy yield, especially when tailored to local irradiance and operational constraints. In addition, recent work by Kumba et al. (2022) [19] investigated second-order lever single-axis solar tracking systems, demonstrating improved energy output over conventional trackers. While partial shading was not specifically studied, the results highlight the potential of optimized mechanical architectures to enhance energy capture under dynamic solar angles. In harsh desert-type climates such as OUED-NECHOU—characterized by high irradiance, dust accumulation, and occasional shading—these design principles are particularly relevant. Building on these concepts, our experiments indicate that optimized single-axis tracking systems, incorporating features inspired by second-order lever architectures, can substantially increase long-term daily energy production. Local factors such as dust storms, ambient temperature fluctuations, and maintenance logistics must guide system selection and operation. Overall, our study confirms that advanced tracking technologies, when adapted to site-specific conditions, can improve energy yield and system resilience in Saharan regions. Recognizing that efficiency and performance are essential aspects of a PV system's functionality, they have been the focus of an extensive body of literature. Numerous studies Pendem and Mikkili., 2018 [21] . Kumar et al., 2018 [22]. Bahanni et al 2020 [23]. Kawajiri et al., 2011 [24] emphasize that various factors, including solar irradiance, ambient temperature, module temperature, wind speed, relative humidity, materials, and the mounting of PV modules. Caouthar Bahanni et al., (2022) [25] conducted a comparative analysis of the energy performance and the influence of meteorological conditions on three photovoltaic technologies (monocrystalline, polycrystalline, and amorphous) installed in two Moroccan cities, Beni Mellal and El Jadida. Using data from one year of operation (January to December 2017), the study assessed the production performance of identical PV stations in distinct climates. The results demonstrated that photovoltaic performance is strongly influenced by meteorological factors. Solar irradiation was identified as the dominant factor, with higher irradiation directly increasing output. Temperature also had a significant impact; rising temperatures led to a reduction in PV cell voltage and power output. Wind speed provided moderate benefits by cooling the panels, slightly improving efficiency, while humidity had the least impact, primarily affecting production through cloud cover. Notably, polycrystalline panels exhibited the highest performance in Beni Mellal, followed by monocrystalline, with amorphous panels being the least efficient. Temperature significantly influences the energy output, power output, and overall efficiency of photovoltaic systems. Amelia et al., (2016) [26] conducted research that conclusively demonstrates that as module temperatures increase, the output power and efficiency of PV panels decrease. Karami et al., (2017) [27] conducted a study on the performance of monocrystalline, polycrystalline, and amorphous solar modules installed on the rooftops of an educational institute in Morocco. The results showed that the maximum performance ratio (PR) achieved was 72.10%, 91.53%, and 86.20% for cloudy days due to low temperature and high wind speed. Conversely, the minimum PR values and PV module efficiency were observed on quiet sunny days and rainy days, impacting the energy generated. The significance of module temperatures in the performance of

solar PV systems is highlighted in the articles by Malvoni et al., (2020) [28]. Al-Maghalseh., (2018) [29], and Kumar et al., (2019a) [30]. To accurately evaluate the performance of PV systems, various models, such as those proposed by Correa-Betanzo et al., (2018) [31] have been suggested for estimating module temperatures. A comparative study by Olukan and Emziane., (2014) [32] examines 16 temperature models based on monthly mean meteorological data. The investigation analyzes how module temperatures fluctuate in response to changes in solar irradiation ranging from 100 to 1000 W/m² and varying ambient temperatures. The results indicate a temperature range for the modules from 31.8 °C to 66 °C across different months. The study emphasizes the performance differences among the models, underscoring the appropriateness of each model for the optimal sizing and design of PV systems. Additionally, Wind speed is a crucial parameter that significantly affects photovoltaic (PV) system performance. While its impact on power production can vary, wind plays a vital role in cooling solar panels, which enhances overall energy output by improving module efficiency. For instance, Balta et al., (2017) [33] observed that consistent wind on PV panel surfaces positively influenced both cooling and the cleaning of dust deposits in Amasya, Turkey. Similarly, Al-Bashir et al., (2020) [34] found that increased wind speed resulted in lower cell temperatures, subsequently boosting output power in PV systems installed in Jordan. Humidity, on the other hand, negatively impacts the performance of PV systems. Water droplets in the air and condensation on panel surfaces diminish the solar irradiation reaching the modules, thereby affecting their efficiency. Ramli et al., (2016) [35] conducted experiments under various weather conditions dusty, cloudy, and rainy in Surabaya, Indonesia, demonstrating performance loss associated with these factors. Furthermore, heightened air humidity often leads to persistent cloud cover, complicating solar energy production. Despite this, humidity remains a significant variable influencing the performance of photovoltaic systems. Building on these findings, numerous studies have explored critical comparisons between fixed and sun-tracking photovoltaic systems, assessing their efficiency, energy yield, and operational effectiveness. Research also includes performance evaluations of PV systems across different climates, large-scale experimental assessments, and the impact of temperature and irradiation on energy production. Furthermore, advanced approaches such as PV cooling techniques and energy-exergy analysis have been examined to enhance system efficiency. Moreover, experimental studies conducted at large-scale PV centers across different regions provide valuable insights into real-world system performance. To effectively highlight key findings, the following literature review table provides a structured summary of relevant studies, emphasizing their contributions to PV system performance analysis and identifying gaps for future research. This tabular presentation systematically outlines the research gaps and the contributions of this study, clearly illustrating the novelty of our work.

Table 1. Literature review table summary of Key Studies on Photovoltaic System Performance

Author (s) Year	Key Findings (Results)	Limitations
Baraa Mahmoud Dawoud, et al ., (2021) [36]	SAT outperformed fixed by 15.08% , SAT enhances energy yield	Excludes real-world factors and economics
Bentouba, Said., et al. (2021) [37]	High temperature effects and performance optimization	Limited to one site, no degradation

Lagouch, A, et al. (2024) [38]	PV performance impacted by climate conditions	Limited site, ignores long-term degradation
Aoun, N.,(2024) [39]	PV efficiency influenced by harsh climate	Lacks PV technology and mitigation analysis
Kumar, N. K.,(2018) [40]	SIST tracking boosts power efficiency	Examines small PV, lacks environmental analysis
Singh, Rajesh, et al., (2018) [41]	Dual-axis tracking boosts energy yield	Literature-based, lacks real-world comparison
Qader, V, et al., (2023) [42]	SAT system outperforms fixed PV	Lacks PR, long-term, limited to short-term performance and seasonal analysis
Kabir, M.H., et al .,(2025) [43]	Dual-axis tracking maximizes solar efficiency.	Lacks PR, long-term and seasonal performance analysis.
Rezk, H., et al., (2019) [44]	OPVP 10MW generated 24.157 GWh efficiently.	10 MW PV monitoring without comparison
Gomaa, Mohamed R., et al., (2020) [45]	Cooling improves PV efficiency and power.	Focus on cooling, ignores other factors
HASHIM, S. M., & HASSAN, R. I. (2022) [46] .	STABLE PV OUTPUT WITH MINIMAL SEASONAL IMPACT	Limited PV study, excludes key factors

This study aims to provide a comprehensive analysis and evaluation of the performance of four photovoltaic subfields, each employing different configurations: two single-axis tracking systems and two fixed systems, incorporating both monocrystalline (mc-Si) and polycrystalline (pc-Si) silicon technologies. Conducted in the Saharan environment of OUED-NECHOU, Ghardaïa, at the SKTM Electricity and Renewable Energy Company unit, this research examines performance under actual weather conditions rather than Standard Test Conditions (STC). The study focuses on key performance metrics, including peak output power (kW), long-term daily power production (kW), and the average daily output power (kW) over each of the four observed days, accounting for seasonal variations. It also evaluates the performance improvement of single-axis tracking systems compared to fixed photovoltaic subfields, with a focus on the gain in output power expressed as a percentage (%). To ensure precise data collection and analysis, daily energy generation (kWh/day) was measured at four-minute intervals. Additionally, this research examines the influence of real-time weather data, recorded at the same intervals, on subfield performance. Key factors include solar irradiation at a 30° tilt (W/m²), ambient temperature (°C), module temperature (°C), wind speed (m/s), and relative humidity (%). The analysis considers seasonal climatic variations and their influence on these meteorological parameters throughout specific experimental days in winter, spring, summer, and fall. A section of this study intends to predict the total solar radiation flux at a 30° tilt using semi-empirical models, specifically the PERRIN DE BRICHAMBAUT model. The expected results will be compared with experimental data recorded in real-time at four-minute intervals over four measured days: January 1st, May 1st, July 1st, and October 1st , each representing a different season. Data was collected from a weather station installed on the roof of the photovoltaic station's control room. Statistical indicators used for comparison between the estimated and measured data include the Absolute Error curve (AE) , Mean Absolute Error (MAE, W/m^2), Root Mean Square Error (RMSE,W/m^2), Correlation Coefficient (CC), and Mean Absolute Percentage Error (MAPE, %). the objective is to determine if the empirical model aligns most closely with the real data based on these statistical tests.

2. Geographical and Meteorological Data of Photovoltaic Power Plants in OUAD-NECHOU, Ghardaïa.

2.1 Geographical Data of OUAD-NECHOU.

The Ghardaïa photovoltaic solar power plant, located in southern Algeria, is part of the renewable energy development program initiated by the supervisory ministry. It is situated near the village of OUED-NECHOU, 15 km north of Ghardaïa along National Road No. 01 as in Fig. 1, with a nominal power capacity of approximately 1100 kWp. The site is bordered by National Road No. 01 to the north and west, and vacant land to the east and south. The plant's precise coordinates are 32°34'43.79'' N latitude and 3°41'55.36'' E longitude, at an altitude ranging from 450 to 566 meters. The closest wilayas are Laghouat and Ouargla. The topography of the site is relatively flat, with a gentle east-west slope.

Ghardaïa's hot, dry climate presents extreme environmental conditions, with temperatures ranging from -5°C to +50°C in the shade. Wind speeds can reach up to 28 m/s, and the maximum recorded relative humidity is 74% at 25°C. Solar irradiations during the summer months can reach 900-1000 W/m². The area also experiences significant temperature fluctuations between day and night 15 to 20°C and frequent winds carrying fine sand

particles, factors critical for plant design and maintenance. Despite these challenges, the plant is located in seismic zone 0, indicating low seismic risk as per Algerian regulations (RPA 99).

Figure 1. Geographical location of the photovoltaic power plants: 1.1 MWp OUED-NECHOU, Ghardaïa City [47].

2.2 Experimental Analysis of Wind Speed (m/s) and Relative Humidity (%) Data Of OUED-NECHOU area.

Researchers and professionals in photovoltaic technology and power plant performance emphasize the importance of understanding regional environmental conditions. Constance Kalu et al., [48] utilize 22 years of meteorological data from NASA's global database, including solar insolation and air temperature, to perform a comparative analysis of polycrystalline, monocrystalline, and thin-film PV technologies using PVsyst version 5.21. Similarly, A. Allouhi et al., [49] employed METEONORM 7 data, including wind velocity, ambient temperature, and solar irradiance, to compare the performance of monocrystalline and polycrystalline PV technologies. Their study evaluates a 2 kWp grid-connected PV plant in Meknes, Morocco, combining recorded data from 2015 and

simulated results to assess the power generation capabilities of these technologies. A. Al-Otaibi et al., [50] assessed the performance of CIGS thin-film PV systems installed on rooftops in Kuwait by monitoring key meteorological parameters such as solar radiation, ambient temperature, wind speed, and module temperature. Using a reference cell and pyranometer for solar radiation measurements, the study recorded data at five-minute intervals over twelve months to evaluate the impact of environmental factors on PV system efficiency in Kuwait's climate.

It is crucial to have accurate weather data to evaluate and optimize the performance of photovoltaic systems. This necessitates using advanced technical instruments to gather experimental data on local weather conditions.

The meteorological station's data acquisition system is installed on the rooftop of the Technical Room at the photovoltaic power plant. It is equipped with devices that provide essential climatic information, including 30° tilted solar irradiance (W/m2), ambient temperature (°C), wind speed (m/s) and direction, and relative humidity (%). Data were collected every 4 minutes from 06:00 AM to 19:52 PM on January 1ST , May 1ST , July 1ST , and October 1ST , representing different seasons (Winter, Spring, Summer, and Fall). Table 2 shows a list and specifications of instruments used by manufacturers.

Table 2. Technical parameters of measuring instruments

Measurement Instruments Parameters	**Thermo-hygrometer**	**Anemometer sensor**	**Pyranometer (Inclined radiation)**
Brand	LSI LASTEM	LSI LASTEM	LSI LASTEM
Model	DMA 672.1	DNA 121#C	DPA 053
County of Origin	Italy	Italy	Italy
Measurements	Relative Humidity (%)	Wind Speed, Direction Outputs	Solar radiation
Measurement range	0 to 100%	0 to 60 m/s	0-1300W/m^2
Precision	3.00%	0 to 3 m/s =1.5 % >3m/s =1%	5 W/m^2
Resolution	0.5 %	0.07 m/s	10 W/m^2

Fig.2. Presents experimental relative humidity data measured with a thermo-hygrometer over four days, from 06:00 AM to 19:52 PM. Each curve corresponds to a different day. The data reveal a consistent diurnal pattern, with higher humidity levels in the early morning and night, decreasing during the day and late afternoon, indicating a regular daily cycle. On October 1st , relative humidity peaked at 90% at 06:00 AM, gradually reducing to 42% by 19:52 PM. A similar trend was observed on January 1st , where humidity started at 67% at 06:00 AM and dropped to 45% by 19:48 PM. On May 1st and July 1st , relative humidity was significantly higher in the early morning, with readings of 42% at 06:00 AM on May 1st and 35% at the same time on July 1st . Throughout the

day,

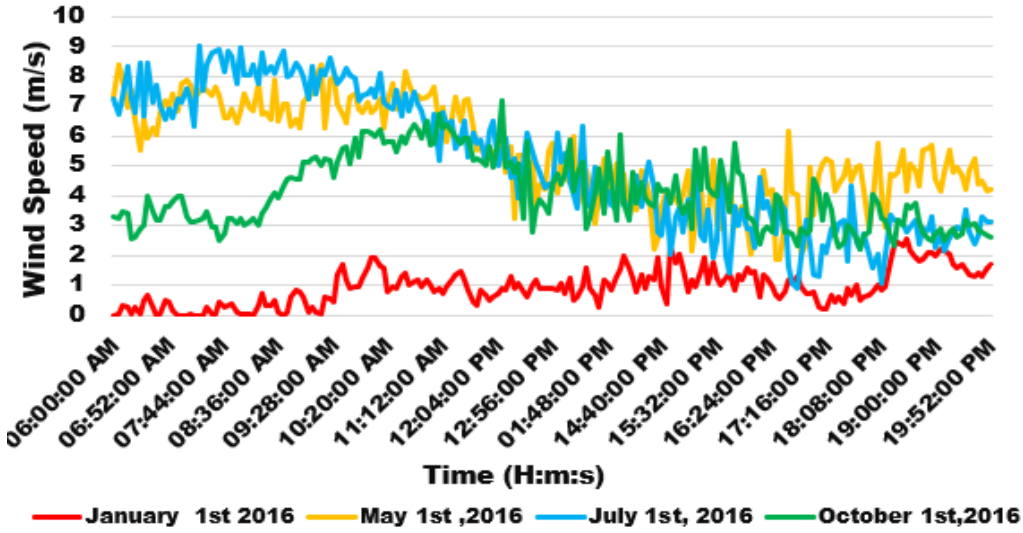

humidity levels steadily decreased, reaching 17% by 19:52 PM on May 1st and dropping to 10% by 19:52 PM on July 1st .

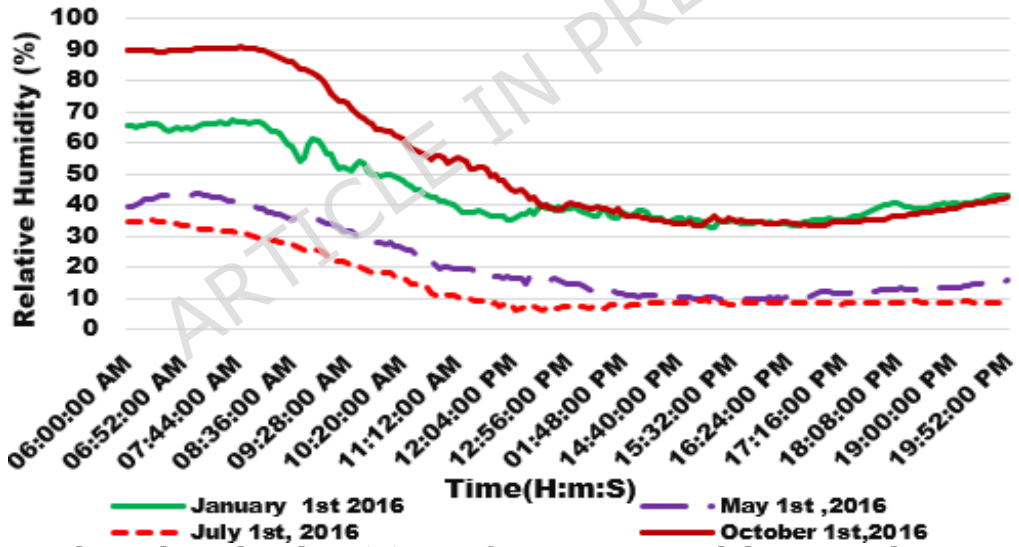

Figure 2. Relative humidity data (%) over four experimental days , each representing a different season in 2016 .

The variation in humidity levels is due to the significant diurnal temperature fluctuations in the OUED-NECHOU region Figures 5-7. Intense heating during the day can lead to very low relative humidity, while in the early morning and at night, temperatures drop sharply, causing a brief rise in relative humidity. The RH data inversely correlates with the daily temperature cycle: as temperature increases, RH decreases, and vice versa.

Figure 3. Wind speed data (%) recorded over four experimental days, each representing a different season in 2016.

Fig. 3. showcases experimental wind speed data from 06:00 AM to 19:52 PM over four days, each curve represents data from a different season, measured using an anemometer.

On January 1st , the wind speed starts at a low of 0.02 m/s at 6:00 AM and reaches a peak of 2.56 m/s in the late afternoon at 6:32 PM. On May 1st , the wind speed peaks at 8.37 m/s in the early morning around 6:04 AM and again at 9:16 AM, then drops to 4.16 m/s by late afternoon around 7:48 PM. On July 1st , the wind speed shows a rapid increase from 7.22 m/s in the early morning at 6:00 AM to 9.05 m/s by 7:24 AM, then decreases rapidly to reach 1.03 m/s, the lowest value recorded on that day, at 6:08 PM. On October 1st , the wind speed peaks at 7.20 m/s around noon and drops to 2.67 m/s by late afternoon at 7:48 PM.

Wind speed changes are influenced by temperature variations. In summer, intense heat from the sahara desert causes air to rise, creating low pressure and stronger winds, as observed on July 1st . In winter, the smaller temperature difference between the desert and surrounding areas leads to weaker pressure gradients and lower wind speeds, as seen on January 1st .

Figs. 2 and 3. Illustrate an inverse relationship between relative humidity (%) and wind speed (m/s) in the OUED-NECHOU region. High wind speeds with low humidity are observed in spring and summer (May 1st and July 1st), while low wind speeds with high humidity occur in winter and fall (January 1st and October 1st). This indicates that as wind speed increases, relative humidity decreases, and vice versa.

3. Theoretical and Measured Setup of Solar Radiation Data on inclined surface 30°

Photovoltaics offer a clean and promising energy solution, making the study of solar resources crucial for this field. A 2017 case study by Bill Marion and Benjamin Smith., [51] developed a method for estimating solar radiation using PV module data with microinverters, validated with data from five systems in Golden, Colorado. The study accurately extracted direct normal irradiance (DNI) and diffuse horizontal irradiance (DHI), which are essential for developing and modeling PV projects in the region.

Various semi-empirical models documented in the literature have been extensively employed to investigate solar radiation on both horizontal and inclined surfaces

A study conducted in Ouargla, which has similar climatic conditions to our study area, OUED-NECHOU in Ghardaïa, was carried out by Abdelmoumen Gougui et al., [52]. The study compared three models (CAPDEROU, PERRIN DE BRICHAMBAUT, and Hottel) for predicting total solar flux on horizontal surfaces using data from a weather station at the LAGE laboratory, Ouargla university. The data was recorded on the 15th of March, April, May, and October. The models were evaluated using RMSE, CC, and MAPE metrics in

MATLAB. The results showed that the PERRIN DE BRICHAMBAUT and CAPDEROU models exhibit greater effectiveness under clear skies in Ouargla, demonstrating a high degree of accuracy and correlation between observed and predicted global solar radiation, this model outperforms the Hottel model. Additional studies on horizontal solar radiation across various regions offer further insights and findings [53-54], [55], and [56].

Abdelatif Takilalte et al., [57] developed a methodology to estimate global tilted irradiation at 5-minute intervals using only global horizontal irradiation data. This approach integrates the PERRIN DE BRICHAMBAUT and LUI & JORDEN models, adjusted for cloudiness factors, to create an anisotropic model. The proposed model demonstrated high accuracy across various metrics, including nRMSE (4.7% to 6.41%), RPE (5.5% to 5.9%), nMAE (3.07% to 4.73%), and R^2 (0.97 to 0.99), especially for short time steps. Compared to conventional and ANN models, the proposed model showed smaller errors, confirming its superior performance. Simultaneously, A. Moummi et al., [58]. conducted a comparative study using data from the Biskra meteorological station to evaluate the PERRIN DE BRICHAMBAUT and LIU & JORDEN models for calculating daily global radiation on an inclined plane. The study found that both models effectively simulated solar irradiance, with the LIU & JORDEN model aligning better with experimental values at sunrise and sunset and the PERRIN DE BRICHAMBAUT model being more accurate around solar noon. This study serves as a reference for our research due to the similar solar radiation patterns in Biskra and OUED-NECHOU and the use of comparable methodologies. Additionally, other studies [59], [60], and [61] have focused on predicting global solar radiation for inclined surfaces, providing results from various regions.

The following excerpt details an experimental comparison study at the 1.1 MWp photovoltaic power plant in OUED-NECHOU, Ghardaïa. A weather station installed on the rooftop of the technical room at the centre of the plant was used to gather authentic data on solar radiation at a 30° tilt. The overall radiation reaching the Earth's surface at this angle includes direct, diffuse, and reflected irradiances as depicted in (1).

$$G_T = S + D_{ciel} + D_{sol} \quad (1)$$

G_T = Global inclined solar radiation [W/m^2].
S = Direct radiation on an inclined plan [W/m^2].
D_{ciel} = Diffuse radiation on an inclined plan [W/m^2].
D_{sol} = Ground reflection radiation on an inclined plan (albedo) [W/m^2].

Experimental real-time data was collected using a pyranometer every 4 minutes, from 06:00 AM to 08:00 PM, over four days in 2016. To estimate the theoretical global irradiance in the OUED-NECHOU region, the PERRIN DE BRICHAMBAUT semi-empirical model was employed, incorporating the linke atmospheric turbidity factor along with atmospheric and astronomical parameters. The equation for global solar irradiance at a 30° tilt was derived using previously obtained geographical data of the region.

Using MATLAB software, the PERRIN DE BRICHAMBAUT model with the Linke atmospheric turbidity factor was applied to simulate the total theoretical inclined irradiance. The results were plotted in Figures 2, 3, 4, and 5 and compared with experimentally inclined irradiances collected over four days representing each season: January 1st (Winter), May 1st (Spring), July 1st (Summer), and October 1st (Fall) of 2016.

The graph displays a comparison of inclined irradiances over four days, featuring the experimental data (red curve) and theoretical data (blue curve). It also highlights the absolute error (yallow curve) between these datasets and presents ambient temperature measurements (green curve) .

Figure 4. PERRIN DE BRICHAMBAUT Estimated Inclined Solar Radiation Compared With Experimental Data on January 1st 2016, A Winter day.

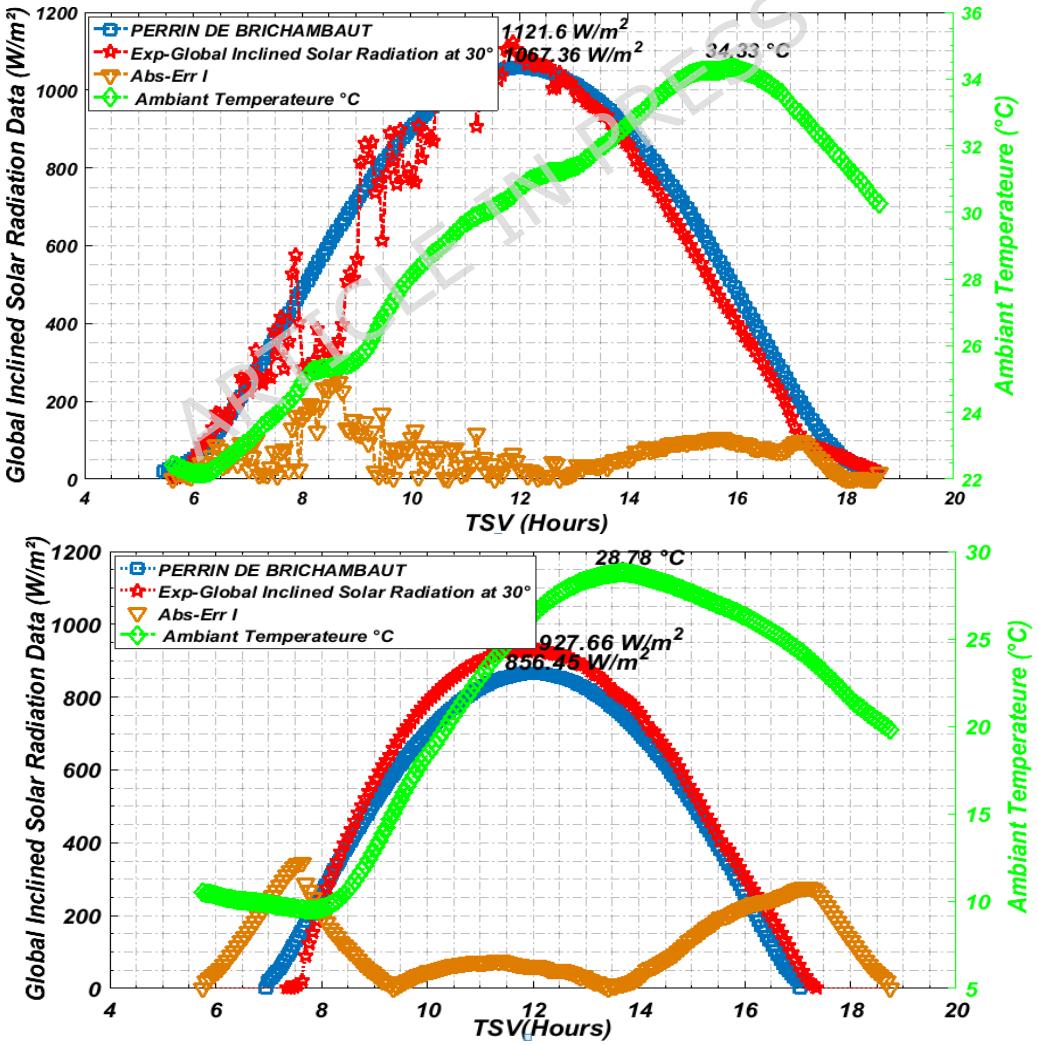

Figure 5. PERRIN DE BRICHAMBAUT Estimated Inclined Solar Radiation Compared With Experimental Data on May 1st 2016, A Spring day.

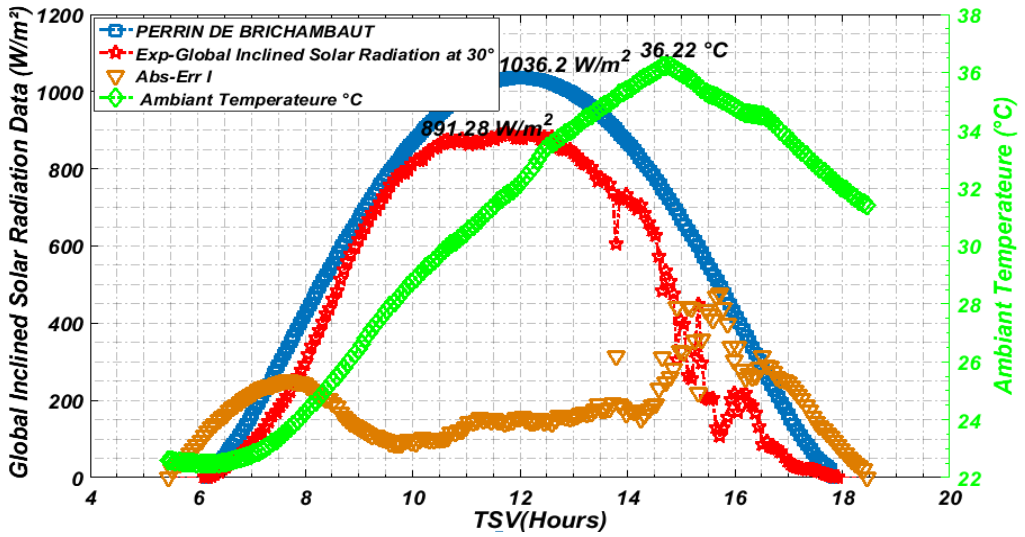

Figure 6. PERRIN DE BRICHAMBAUT Estimated Inclined Solar Radiation Compared With Experimental Data on July 1st 2016, A Summer day.

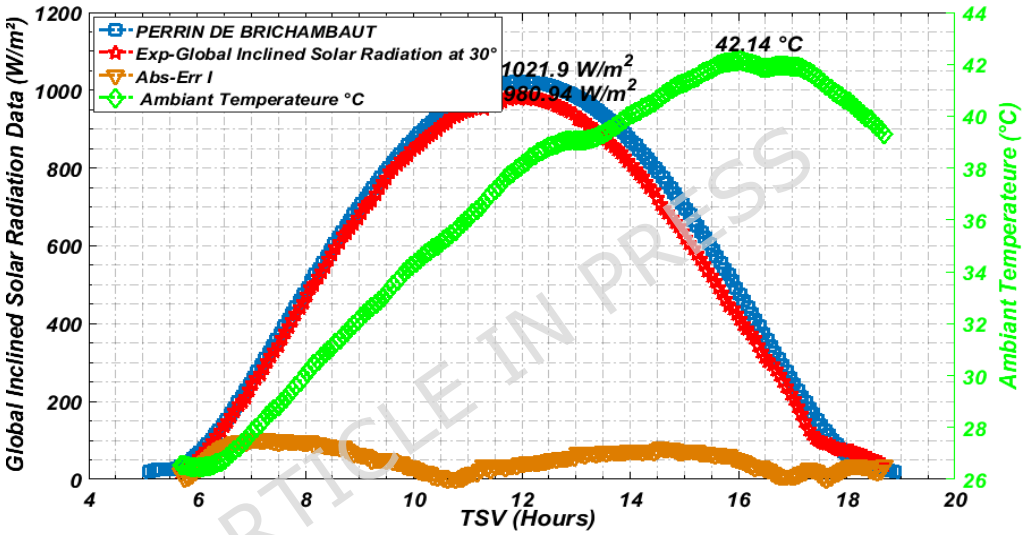

Figure 7. PERRIN DE BRICHAMBAUT Estimated Inclined Solar Radiation Compared With Experimental Data on October 1st 2016, A Fall day .

The solar irradiance results show a strong correlation between measured and predicted data on January 1st (a winter day) and October 1st (a fall day), particularly at sunrise, sunset, and midday. On January 1st , the experimental peak solar irradiance was 927.61 W/m², with a predicted value of 865.45 W/m² around midday. On October 1st , the maximum measured value was 1021.9 W/m², while the estimated value was 980.94 W/m².

On May 1st (a Spring day), there was a fluctuation in the experimental solar irradiance data compared to the estimated data from 6:00 AM to 12:00 PM. This fluctuation was due to a sharp increase in wind speeds, as shown in Fig. 3, where the highest value recorded by the anemometer sensor reached 8.37 m/s, resulting in instability in the inclined solar radiation during that time. However, from 12:00 PM to 6:00 PM, there was consistency between the experimental and estimated data. The highest value for experimental solar radiation was 1121.6 W/m², while the estimated solar radiation was 1057.3 W/m², both recorded around midday.

On July 1st (a summer day), we observed consistency between the measured and estimated data from 6:00 AM to 10:00 AM. However, from 10:00 AM to 6:00 PM, disturbances began to appear in the real solar radiation data. These disturbances were due to the changing wind speeds and the presence of clouds, which prevented the passage of solar radiation. The wind speed data on this day was the highest among the four experimental days, with the anemometer sensor recording a maximum of 9.05 m/s. Furthermore, the maximum measured value of solar irradiance was 891.28 W/m², while the estimated value was 1036.2 W/m².

In their study of solar radiance in Biskra, A. Moummi et al., [58] concluded that variations in solar radiation data throughout the day are primarily due to climatic disturbances. Similarly, Benbouza Naima et al., [62] demonstrated through images in her study of solar radiation in Batna, Algeria, that several natural factors, including wind and clouds, can significantly affect solar radiative flux, leading to instability in the collected data.

The performance of the semi-empirical model was validated using statistical parameters [63], including MAE, CC, RMSE, MAPE, and the absolute error curve. These indicators are commonly used in the comparison and assessment of solar radiation models, as highlighted in the literature [52-60, 66-65]. The results of the statistical analysis over four experimental days are shown in Table 3.

Table 3. Statistical Test Values for the PERRIN DE BRICHAMBAUT model over four experimental days in 2016.

Days	MAE(w/m²)	RMSE(w/m²)	CC	MAPE (%)
January 1st,2016	65.9448	7.7183	0.8273	4.1243
May 1st, 2016	55.5830	5.0292	0.6469	8.8694
July 1st, 2016	52.2668	4.2737	0.9668	1.9684
October 1st , 2016	61.6452	6.6486	0.9491	4.649

The statistical indicators (MAE, RMSE, CC, and MAPE), evaluated over four days in 2016, demonstrate that the PERRIN DE BRICHAMBAUT semi-empirical model closely matches the actual data .

July 1st (a summer day) provides the best accuracy for the solar radiance predictions based on the MAE values, with an MAE of 52.2668 W/m² . This reflects the smallest average error in the predictions compared to the other days analyzed, indicating superior predictive accuracy. Furthermore, on July 1st , the model achieved its highest accuracy with the lowest RMSE of 4.2737 W/m², reflecting close alignment between predicted and actual solar radiance values and demonstrating strong performance. The more, the correlation coefficient (CC) of the model is consistently high, exceeding 0.7 over the four measured days, with the highest value of 0.9668 observed on July 1st . This high CC value

indicates a strong correlation between observed and estimated solar radiance in tilt of 30°.These results suggest that the model performs well in correlating observed and estimated values across all days, demonstrating robust predictive capability. The MAPE, which quantifies accuracy as a percentage, shows excellent results with values below 10% for all days. The best performance was observed on July 1st , with a MAPE of 1.9684%, highlighting the model's robustness and reliability in estimating inclined solar irradiance.

We can confidently conclude that the PERRIN DE BRICHAMBAUT model provides a good fit and correlation between measured and predicted global solar radiation over four observed days. The model is particularly effective for regions with latitudes below 60°, in line with findings from the Atlas Solaire de l'Algérie [66]. Therefore, this semi-empirical model can be used to predict global inclined solar radiation at a 30° tilt in photovoltaic power plants in OUED-NECHOU, Ghardaïa, even in the absence of a pyranometer instrument.

4. Description of the photovoltaic installation at the photovoltaic power plants in OUED-NECHOU, Ghardaïa.

The power plant, constructed by S.P.E. (Algerian Electricity Production Company), is located approximately 15 km north of Ghardaïa, near the village of OUED-NECHOU. The site spans ten hectares and houses a photovoltaic plant designed to harvest and directly convert sunlight into electricity.

With a nominal power of approximately 1100 kWp, the plant aims to evaluate the performance of various photovoltaic technologies in the southern Algerian environment, where conditions such as high solar radiation and temperature extremes can significantly impact efficiency. This pilot project is divided into eight sub-fields, each containing four photovoltaic modules of different technologies and two types of structures (fixed and motorized). The installation is oriented towards the south (azimuth angle = 0°) and inclined at an angle of 30°.

The Table below represents the central constitution of the photovoltaic power plants at OUED-NECHOU, Ghardaïa distributed as follows:

Fig.8. provides an overview of the PV accessory center at OUED-NECHOU, showcasing the primary photovoltaic technologies present at the site.

- Monocrystalline silicon panels (452 kWp).
- Polycrystalline silicon panels (452 kWp).
- Amorphous silicon (a-Si) panels (100 kWp).
- Thin film panels (cadmium telluride CdTe) (100 kWp).

These images were obtained during an experimental study conducted at the center .

Figure 8. Illustrative Image of the OUED-NECHOU Photovoltaic Power Plant in Ghardaïa, showing its PV Subfields Inclined at 30° Facing South

This study presents an experimental comparison of four photovoltaic subfields configured as two fixed and two single-axis tracking systems, all inclined at 30°. Each subfield consists of a series-connected array of photovoltaic modules, with each subfield having a

capacity of approximately 100 kW. The objective is to evaluate the performance of these photovoltaic technologies, specifically monocrystalline silicon (mc-Si) and polycrystalline silicon (pc-Si), which share identical material compositions but differ in structural configuration. The experiment was conducted over four days under identical meteorological conditions at the OUED-NECHOU site, with specific climatic conditions representative of southern Algeria. Detailed technical parameters are provided below.

a)- Sub-field (1) has a capacity of 105 kWp and features a motorized monocrystalline silicon (mc-Si) structure. The peak power output of each photovoltaic (PV) panel is 250 Wp. This sub-field comprises 420 photovoltaic modules, organized into 21 chains, with each chain consisting of 20 modules.

b)- Sub-field (2): has a capacity of 98.7 kWp with a Motorized polycrystalline silicon structure (pc-Si), and the peak power output of the PV panel is 235 Wp. This sub-field comprises 420 photovoltaic modules, organized into 21 chains, with each chain consisting of 20 modules.

c)- Sub-field (3) has a capacity of 108 kWp with a fixed thin- film structure using Cadmium Telluride (CdTe), and the peak power output of the PV panels 80 Wp .This sub-

field comprises 1260 photovoltaic modules, organized into 105 chains, with each chain consisting of 12 modules.

d)- Sub-field (4): has a capacity of 100,116 kWp with a fixed amorphous silicon structure (a-Si), and the peak power output of the PV panel is 103 Wp .This sub-field comprises 972 photovoltaic modules, organized into 54 chains, with each chain consisting of 18 modules.

e)-Sub-field (5) has a capacity of 105 kWp with a Fixed monocrystalline silicon structure (mc-Si), and the peak power output of the PV panel is 250Wp.This sub-field comprises 420 photovoltaic modules, organized into 21 chains, with each chain consisting of 20 modules.

f)-Sub-field (6): has a capacity of 98.7 kWp with a Fixed polycrystalline silicon structure (pc-Si), and the peak power output of the PV panel is 235 Wp. This sub-field comprises 420 photovoltaic modules, organized into 21 chains, with each chain consisting of 20 modules.

5. Design of Fixed and Tracking Support Structures for Photovoltaic Panel Installations.

Being an experimental site, the Ghardaïa photovoltaic plant was chosen to use four different types of panels and two types of support structures: fixed structures or mobile (motorized tracking systems).

The subfields containing either fixed structures or automated tracking systems are

discripted above Either the fixed structures or the motorized structures will be installed on the ground through concrete blocks. The structures will be made of galvanized steel, and sized in accordance with site conditions. The fixed structures will be oriented towards the south with a tilt angle of 30°, to optimize the sunshine on the panels see Fig.9.

Figure 9. Fixed Structure of the Photovoltaic System in the OUED-NECHO Subfields for Monocrystalline (mc-Si) and Polycrystalline (pc-Si) Technologies.

The tracking systems will be of the single-axis type, with the axis oriented in the east-west direction. Throughout the day, the tracker follows the sun's movement from sunrise to sunset, using (azimuthal tracking) from east to west . The panels installed on the tracker will be tilted at a 30° angle to enhance sunlight capture. This configuration maximizes the angle of incidence of sunlight on the panels throughout the day, thereby improving the efficiency and power output of the photovoltaic system compared to fixed-tilt systems. Additional details about the motorized structures are shown in Fig. 10.

Each tracker is moved by an electric motor located on the system and powered by a low voltage (LV) panel of the power plant. Fig.11.

The movement of the tracking systems is synchronized by a proprietary control system (PLC). Tracking systems will need to return the modules to horizontal for high wind speed.

Figure 10. Single-Axis Tracking Structure of the Photovoltaic System in the OUED-NECHO Subfields for Monocrystalline (mc-Si) and Polycrystalline (pc-Si) Technologies.

Figure 11. Motorized Tracking System for the PV Subfields (SLAVE).

6. Experimental Setup, System Configuration, and Data Acquisition

The functional operation of the single-axis tracking system, as illustrated in Fig. 10 and Fig. 11, is described as follows:

During operation, the tracking mechanism followed a stepped movement protocol: each drive chain was activated for approximately 5 s, followed by a 10-minute rest period, in sequential order across 21 chains. This gradual motion minimized actuator wear and reduced energy consumption. Position control relied on mechanical limit switches and predefined end stops, as the system lacked high-resolution encoders due to its legacy design. This stepped strategy provided near-continuous sun-following while significantly reducing motor duty cycles. The mechanical drive employs a toothed gearing system composed of an electric motor and meshing gear teeth.

Data collection was conducted using the central PV monitoring system, which logged DC output power, tracker motion events, and meteorological variables at 4-minute intervals from sunrise to sunset. Pyranometers and temperature sensors were visually inspected and zero-adjusted according to manufacturer guidelines prior to the measurement campaign. Sensor readings were periodically cross-checked, and tracker alignment was verified at predefined timestamps to ensure accuracy and reliability of measurements.

7. Technical Characteristics of Photovoltaic Technologies

The electrical characteristics of the PV modules at standard testing conditions (1000 W/m², 25 °C, AM1.5) are detailed in Table 4. Both monocrystalline and polycrystalline

technologies adhere to the same manufacturer's specifications for tracking and fixed systems.

Table 4. PV Modules Technical Specifications

Photovoltaic Technologies	Monocrystalline (mc-Si)	Polycrystalline (pc-Si)
Type	ATERSA A-250M	ATERSAA-235P
Peak power	250Wp	235 Wp
Peak power tolerance	0 / +5 Wp	0 / +5 Wp
Module performance	15.35%	14.43%
Max voltage (Vmpp)	30.35 V	29.04 V
Max intensity (Impp)	8.24 A	8.10 A
Surface (m^2)	1.63	1.63
Open circuit voltage (V)	37.62 V	36.94
Short circuit current	8.79 A	8.64 A
Max system voltage	1000 V	1000 V
NOCT	47 +/- 2 [°C]	47 +/- 2 [°C]
Temperature coefficient Isc	+0.03% [K]	+0.04% [K]
Temperature coefficient Voc	- 0.34% [K]	- 0.32% [K]
Temperature coefficient Pmax	-0.43% [K]	-43% [K]
Weight	21.5 kg	21.5 kg
Dimensions	1645 x 990 x 40 mm	1645 x 990 x 40 mm
Cells	60	60

8. Performance Assessment Methods for Photovoltaic Subfields

In this section, we will evaluate four critical aspects of the performance of photovoltaic (PV) subfields: I) Output Power, II) Environmental Factors Influencing Performance, III) Augmentation Percentage, and IV) Daily Energy Yield. The primary objective of this assessment is to identify which PV subfield demonstrates the highest performance and is the most suitable for installation in regions with desert climatic conditions, such as the OUED-NECHOU region in Ghardaïa City.

7.1 Peak Output Power (KW) and Long-term Daily Performance

To evaluate photovoltaic module performance, a simulation approach was conducted by Constance Kalu et al.,[48]. Using PVsyst version 5.21 and NASA meteorological data along with hypothetical load demand, the study compares polycrystalline, monocrystalline, and thin-film PV technologies. It finds that thin-film PV technology, despite its low array loss, low unit cost of energy, and favorable performance metrics, requires a larger installation area. In contrast, polycrystalline PV technology, with higher efficiency and smaller space requirements, is deemed more suitable for the specific site due to its superior efficiency and compact space needs. Furthermore, Allouhi et al., (2016) [46] assessed the performance, economic feasibility, and environmental impact of 2 kWp grid-connected PV systems (Poly-Si and Mono-Si) installed at the High School of Technology, Meknes, Morocco. The two PV fields are oriented south at a fixed tilt angle of 30°. Using METEONORM data and PVSYST simulations, the study found Poly-Si modules slightly outperform Mono-Si, with a higher annual average daily final yield. The Meknes systems perform better than those in Greece, Ireland, India, South Africa, and the UAE. Economically, Poly-Si has a lower levelized cost of electricity ($0.073/kWh) and shorter payback time (11.10 years) compared to Mono-Si ($0.082/kWh and 12.69 years). The systems also offer significant environmental benefits, reducing CO2 emissions by

about 5.01 tons annually. The International Electrotechnical Commission (IEC) recommends several parameters for assessing PV power plant performance, as outlined in IEC-61724 standards. Key parameters include the final yield (Yf), reference yield (Yr), performance ratio (PR), and capacity factor (CF) Cubukcu & Gumus., 2020 [67]. Pirzadi & Ghadimi ., 2020 [68]. Veerendra Kumar et al., 2022 [69]. Ismail Bendaas et al., 2023 [70] . IRFAN JAMIL et al.,2022 [71] [61-67]. These indicators are crucial for evaluating the efficiency and profitability of various PV power plants under different climatic conditions and for detecting potential issues or failures. Building on this. El Mehdi Karami et al., (2018) [72] evaluated the performance of grid-connected PV systems with monocrystalline, polycrystalline, and amorphous silicon modules in Casablanca, using 2016 data and PVsyst simulations. They assessed performance parameters such as annual energy generation, final yield, reference yield, performance ratio, and capacity factor. Results indicated that simulations were accurate for energy production and irradiation but less accurate for ambient temperature. Performance ratios were 76.94% for p-si, 78.02% for c-si, and 67.28% for a-si, with final yields of 4.61, 4.68, and 4.02 kWh/kWp/day, respectively. The study confirms PVsyst's reliability but suggests using on-site temperature measurements for better simulation accuracy.

Assessing solar panel performance by analyzing output power, a critical electrical parameter, is essential for comparative studies, especially when considering the specific meteorological conditions of a given location. El Mehdi Karami et al., (2018) [72] conducted additional research to evaluate the performance of different solar panel technologies. They assessed the DC power output from the modules and the AC power from the inverters using real-time measurements under various weather conditions clear, cloudy, and rainy. Additionally, Layachi Zaghba et al., [73] conducted an experimental study on an 11.28 kWp grid-connected solar system with sun tracking over one year at the Applied Research Unit of Renewable Energy in Ghardaia, Algeria. The study combines simulation data from PVSYST with experimental results and features three 3.76 kWp solar tracker configurations: fixed-axis, one-axis, and dual-axis. In a specific section, it compares the power output of single-axis and dual-axis trackers with fixed-axis systems under varying weather conditions, including clear and cloudy skies. Arechkik Ameur et al.,[74] aimed to analyze and compare various indices for evaluating the performance of three grid-connected photovoltaic technologies (a-Si, pc-Si, and mc-Si) in Ifrane, Morocco, at Al Akhawayn University. The study examines systems generating 2 kWp each, installed facing south on a flat surface, tilted at 32°, with zero azimuth. It evaluates AC power output under sunny and snowy conditions, considering the impact of temperature on power output.

Two different crystalline silicon photovoltaic technologies, monocrystalline silicon (mc-Si) and polycrystalline silicon (pc-Si), were evaluated using two types of support structures: fixed-axis and single-axis, both with a 30° tilt. Each PV subfield consisted of identical 100 kWp systems. Data were collected every 4 minutes in real-time through field measurements, as illustrated in Fig.12–15. A comparative analysis was conducted. On the peak output power and long-term daily power generation for January 1st , May 1st , July 1st , and October 1st , representing the four seasons.

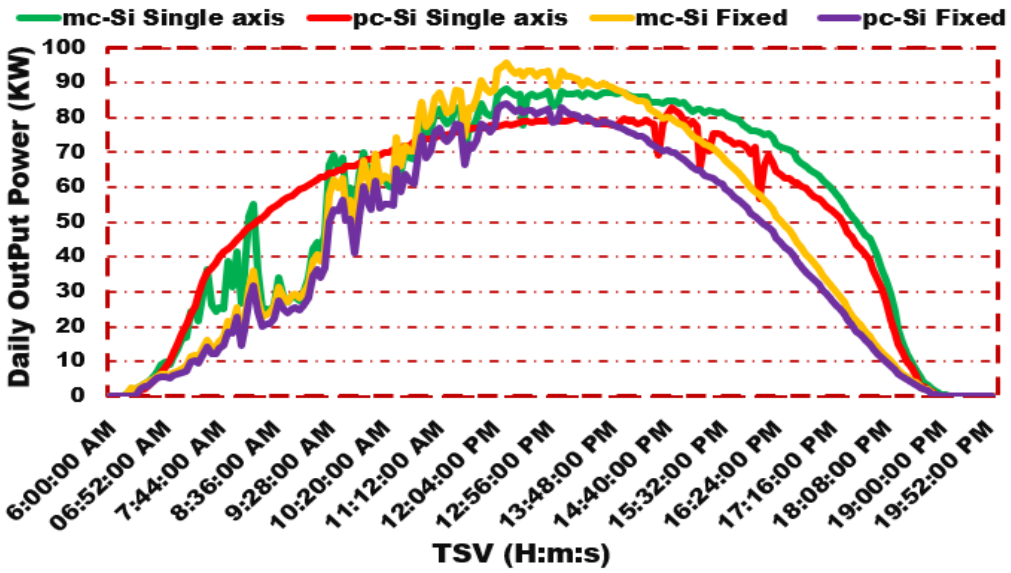

Figure 12. Comparison of Output Power (kW) Between Fixed and Single-Axis PV Subfields for mc-Si and pc-Si on January 1st , 2016. A Winter Day .

After confirming the accuracy of the PV subfields' real performance data. Fig.12.Shows the power output of the fixed-axis and one-axis mc-Si and pc-Si subfields on a winter's day in January 1st , 2016. Around 12:58 PM, the fixed mc-Si subfield reached its peak of 82.31 kW, the highest output of the day. Earlier, at 10:37 AM, the motorized mc-Si subfield produced 75.10 kW . Past midday the fixed pc-Si subfield generated 73.98 kW at 12:57 PM, while the motorized pc-Si recorded the lowest output of 73 kW at 10:50 AM.

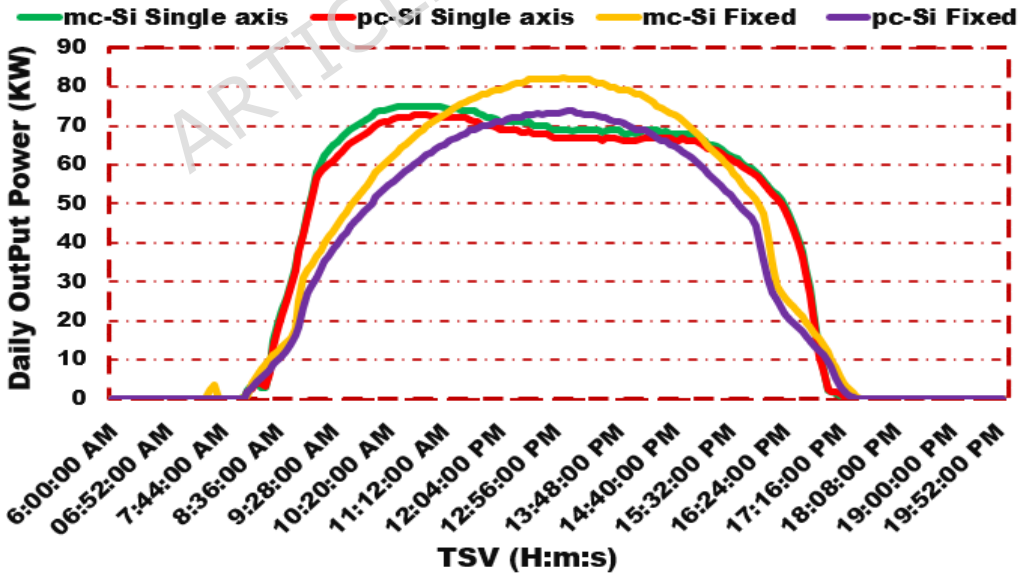

Figure 13. Comparison of Output Power (kW) Between Fixed and Single-Axis PV Subfields for mc-Si and pc-Si on May 1st , 2016. A Spring Day .

The findings from the four PV subfields on May 1st , 2016, a spring day, are displayed in Fig. 13.Showing the maximum power output recorded during the four-day pilot study. At 12:23 PM, the fixed mc-Si subfield achieved the highest power output ever recorded, approaching 95.67 kW .This was followed by the motorized mc-Si subfield, which produced 88.35 kW at 12:20 PM . At the same time, the fixed pc-Si subfield produced

84.06 kW, while the motorized pc-Si subfield recorded the lowest output of 83.01 kW at 14:40 PM.

Figure 14. Comparison of Output Power (kW) Between Fixed and Single-Axis PV Subfields for mc-Si and pc-Si on July 1st , 2016. A Summer Day .

Fig. 14. illustrates the comparison of output power curves from four subfields one -axis and fixed-axis mc-Si and pc-Si using real data from July 1st , a summer day. The

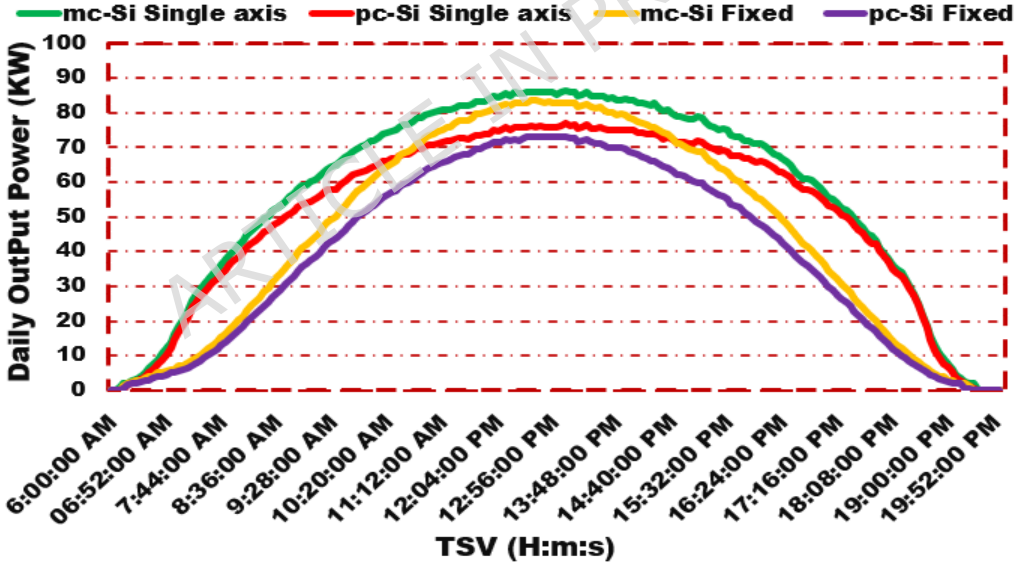

experimental results on this day differed from those of the previous day. The one-axis mc-Si subfield yielded the highest power output on this day, producing 86.38 kW at 12:56 PM. This was followed by the fixed mc-Si subfield, which generated 83.84 kW at 12:46 PM. The motorized pc-Si subfield produced 76.84 kW at 13:28 PM, while the fixed pc-Si subfield achieved 71.12 kW.

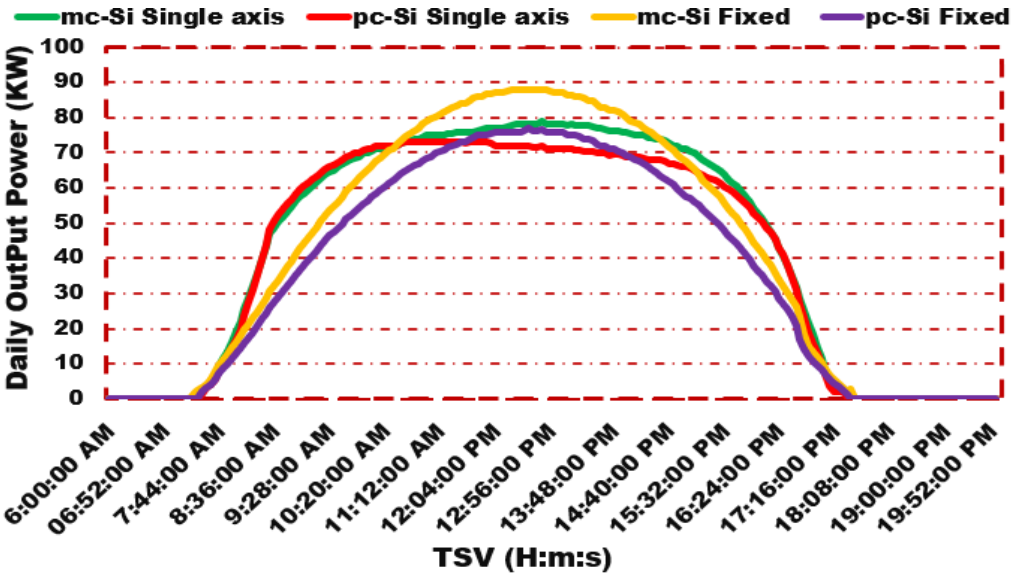

Figure 15. Comparison of Output Power (kW) Between Fixed and Single-Axis PV Subfields for mc-Si and pc-Si on October 1st , 2016. A Fall Day .

Fig. 15. Presents experimental real data on output power for fixed-axis and one-axis PV subfields from October 1st , 2016, covering a full day. The curves reveal that the fixed-axis mc-Si subfield yielded the highest output power compared to other subfields, achieving 88.00 kW at 12:56 PM. Following this, the one-axis mc-Si subfield delivered 78.79 kW at 13:05 PM . Additionally, the performance comparison between the fixed and single-axis pc-Si subfields shows a relatively close peak output, with the fixed pc-Si subfield achieving 76.88 kW and the single-axis pc-Si subfield reaching 73.06 kW at 10:50 AM.

When comparing the DC output power performance of four conventional PV subfields in this section, the results from four experimental days indicate that on each of these days, the power output of the solar panels was monitored from sunrise to sunset, between 06:00 AM and 19:52 PM. Among the subfields, the fixed monocrystalline (mc-Si) consistently generated the highest output power, with a peak value of 95.67 kWp recorded on May 1st , close to the subfield's optimal capacity. Additionally, on the same day, the single-axis monocrystalline (mc-Si) subfield demonstrated a peak output power of 88.35 kWp.

Notably, the single-axis solar tracker consistently increased the amount of power generated throughout all experimental days, from sunrise to sunset, by capturing more solar radiation compared to a fixed module. This effect was particularly evident on January 1st , May 1st , and July 1st . As a result, by implementing single-axis tracking systems in our mc-Si and pc-Si subfields, the PV panels were able to continuously track the sun. These systems ensure that the panels remain optimally aligned with the sun throughout the day and across the year, maximizing the exposure of the panel’s surface. This alignment leads to increased conversion efficiency and, consequently, higher electricity generation (output power). Additionally, tracking systems optimize land area usage for electricity production compared to non-tracking systems, making them a more efficient choice. This finding is consistent with those obtained by many authors who have studied solar tracking systems. Hafez et al. (2015) [75] introduced an innovative solar single-axis tracking system powered by a Stirling engine, which was used to evaluate the performance of solar panels in Giza, Egypt. The East-West axis system achieved higher output power than the fixed system. Research carried out by Layali Abu Hussein et al. (2021) [76] in Amman, Jordan, looked into the performance improvement of standard fixed photovoltaic (PV) solar systems by using single and dual-axis sun tracking mechanisms. They compared these systems to concentrated photovoltaic (CPV) systems, which inherently use tracking systems. The study included an experimental analysis, characterization, and performance comparison of four mounting types of standard PV systems. The PV panels were installed using either a fixed mount, single-axis (East-West tracking), single-axis (North-South

tracking), or dual-axis tracking. The study's findings confirmed that electrical power generation on tracking surfaces was significantly higher than on a fixed surface. Additionally, the study demonstrated that both East-West and North-South tracking systems produced more power compared to a fixed surface inclined at 26° to the south.

7.2 Influence of Environmental Factors (Solar Irradiance at 30° Tilt, Temperature, Wind Speed, and Relative Humidity) on Subfield Performance.

Climatic, environmental, and operational conditions, along with geographical locations, play a crucial role in the energy yield of photovoltaic (PV) systems. This concept has driven research focused on quantifying and modeling the output power of PV systems under diverse conditions. Researchers globally aim to understand better how these parameters affect PV system performance. According to Elkholy et al., (2016) [77], reduced solar irradiation significantly influences the energy quality produced by photovoltaic systems .Dabou et al., (2016) [78], conducted a study examining the impact of climatic conditions on the performance of grid-connected photovoltaic systems. The findings indicate that performance is influenced on cloudy and sandy days due to the rapid and successive changes in cloud cover and sand exposure, which affect both the energy output and the stability of the photovoltaic system. In their 2014 study, Panagea et al [79] . discovered a clear inverse link between PV power and temperature in Greece. They also observed that as irradiance intensity rises, so does PV power. As reported by Schwingshackl et al., (2013) [80] and Kaplani and Kaplanis (2014) [81], wind speed significantly enhances PV performance by cooling the PV surfaces, which in turn reduces the parallel resistance within the PV circuit model. Humidity decreases PV output by diminishing the amount of solar irradiance received. Nevertheless, when combined with wind speed, humidity significantly contributes to cooling PV surfaces, thereby enhancing PV efficiency in hot climates Zainuddin et al., 2010 [82].

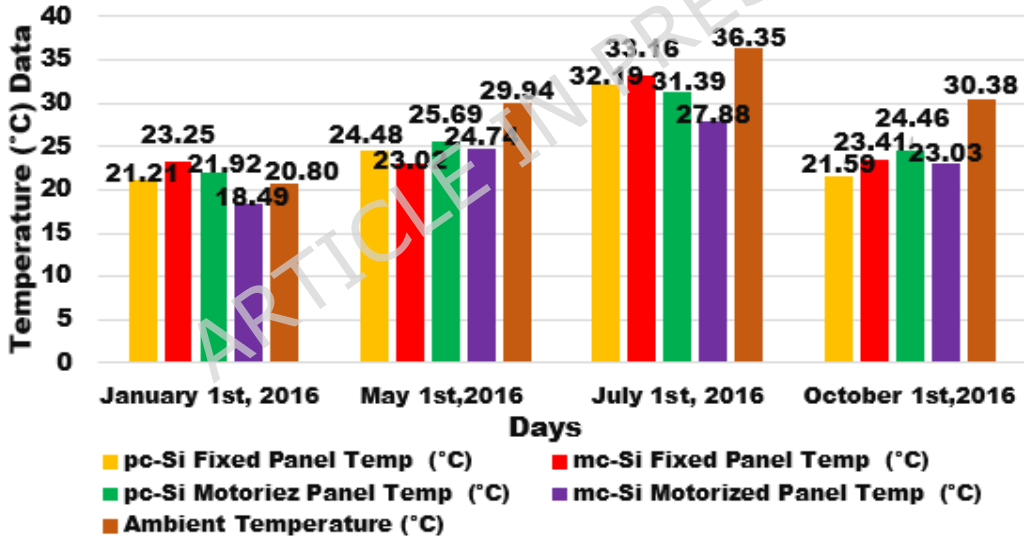

Currently, no published studies provide experimental results on the performance of photovoltaic systems and their interaction with environmental factors in the OUED-NECHOU region, Ghardaïa. This section presents a comparative analysis of the influence of meteorological parameters on photovoltaic subfield performance based on experimental data. The study evaluates the effects of solar irradiance at a 30° tilt, cell irradiation at the same angle, ambient temperature, cell temperature, relative humidity (Fig. 2), and wind speed (Fig. 3) on the DC power output. Furthermore, the performance of both fixed and motorized (single-axis) subfields is analyzed to determine which technology is more effective under these environmental conditions. Real-time meteorological data was collected using sensors installed at a weather station (Table 1) on the roof of the control room, recorded at four-minute intervals on January 1st , May 1st , July 1st , and October 1st each representing a different season. The data was displayed and analyzed, as shown in Figures 2, 3, 16, and 17.

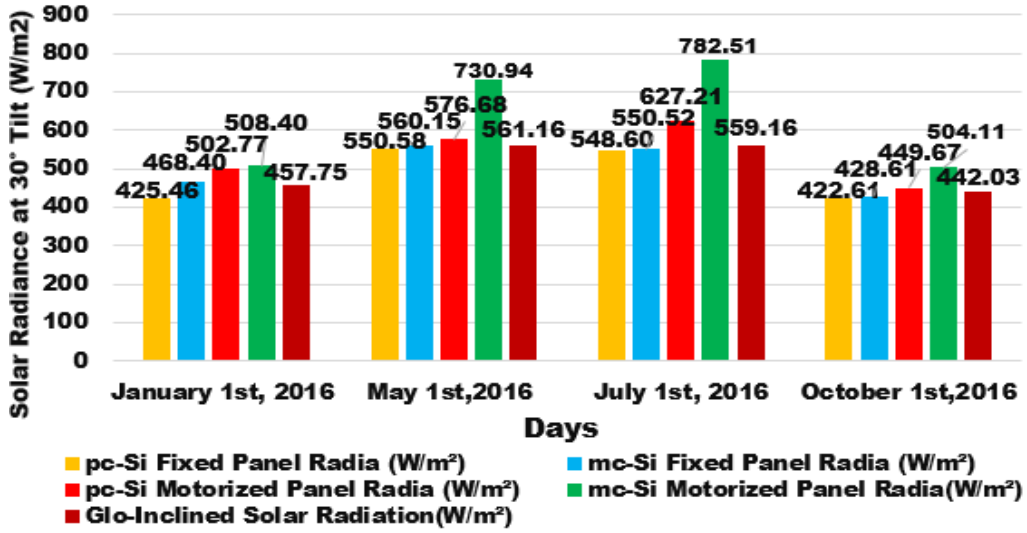

Figure 16. Daily Experimental Data of Average Ambient Temperature (°C) and Module Temperature (°C) Over Four Days, Each Corresponding to a Different Season.

Fig. 16. Compares experimental data from four days, including ambient temperature recorded by a thermo-hygrometer installed at the weather station and PV module temperature from both fixed and motorized technologies, measured by cell sensors installed in the subfields. Data analysis revealed that ambient temperatures consistently exceeded the temperatures recorded by the PV cell sensors throughout the four experimental days. PV module temperatures also increased with rising ambient temperatures, with the most significant effect observed on July 1st .

The fixed mc-Si technology reached its peak panel surface temperature of 33.16°C on July 1st and its lowest of 23.02°C on May 1st , while the fixed pc-Si PV technology recorded its highest at 32.19°C on May 1st and its lowest at 21.21°C on January 1st . These distinct temperature changes vividly illustrate the seasonal performance variations of these PV technologies. On July 1st , mc-Si and pc-Si one-axis panels recorded their maximum average temperatures of 27.88°C and 31.39°C, respectively, while on January 1st , they had their minimum averages at 18.49°C and 21.92°C.

Figure 17. Daily Experimental Data of Average Inclined Solar Irradiance (W/m²) and Calibrated Cell Radiation (W/m²) For Four Subfields Over Four Days, Measured at a 30° Tilt Angle.

Fig. 17. Showcases an experimental comparison of inclined solar irradiance (W/m²) recorded by a pyranometer and measured by calibrated cells, both positioned at a 30° tilt angle over four days representing different seasons.

Significant emphasis was placed on the clear and qualitative response of the subfields to different levels of solar radiation. The motorized mc-Si and pc-Si subfields outperformed the fixed subfields and the pyranometer in capturing solar radiation

On July 1st , a summer day, the monocrystalline silicon (mc-Si) technology recorded a peak average solar irradiance of 782.51 W/m², the highest observed during the study. In contrast, the lowest value, 504.11 W/m², was recorded on October 1st , a fall day. On January 1st , a winter day, the irradiance was 730.94 W/m², while on May 1st , a spring day, it was 508.41 W/m². The motorized pc-Si subfield also achieved significant irradiance values, with a maximum average of 627.21 W/m² on July 1st . On May 1st , it recorded 576.68 W/m². During winter (January 1st) and fall (October 1st), the irradiance values were 502.77 W/m² and 449.67 W/m², respectively.

On May 1st , the pyranometer recorded a maximum average solar irradiance of 651.16 W/m². The fixed mc-Si sub-field recorded an average irradiance of 560.58 W/m², which is 90.58 W/m² lower than the pyranometer's measurement. The fixed pc-Si subfield recorded a maximum irradiance of 550.58 W/m², showing a difference of 100.58 W/m² from the pyranometer's reading. In October, the pyranometer recorded the lowest tilted solar irradiance values in this study, with a minimum of 442.03 W/m². The fixed mc-Si subfield measured 428.61 W/m², 13.42 W/m² lower than the pyranometer's reading, while the fixed pc-Si subfield recorded 422.61 W/m², 19.42 W/m² below the pyranometer's measurement.

These measurements illustrate the variability in irradiance captured by different PV technologies, highlighting the pyranometer's role as a benchmark for evaluating the performance of photovoltaic subfields in capturing solar radiation.

The experimental results indicate that one-axis solar subfields consistently generate more power from sunrise to sunset compared to fixed subfields. This increased power production was particularly evident on January 1st , May 1st , and July 1st . The east-west alignment of single-axis panels optimizes solar energy absorption by optimizing the polarization angle of incoming solar radiation.

Natural factors clearly influence this variation in power production. Extensive studies have proven this, including those by Karami et al., (2017) [27]. Al-Otaibi et al., (2015) [50], and Moafaq K.S. et al., (2022) [83]. Layali Abu Hussein et al .,(2021) [76]. At the OUED-NECHOU station, the tilt angle of the solar panels plays a crucial role in determining photovoltaic subfield efficiency. A well-adjusted tilt that aligns closely with the region's optimal angle improves solar energy absorption and enhances power generation. Observations on May 1st and July 1st revealed that single-axis subfields benefited the most from increased solar irradiance, resulting in notable power gains [76]. On July 1st , the motorized panels recorded peak solar radiation values of 782.51 W/m² for mc-Si and 625.51 W/m² for pc-Si, highlighting their ability to maximize power generation compared to fixed panels. During the experimental study, the average temperatures of the photovoltaic (PV) technologies remained close to the optimal Standard Test Condition (STC) of 25°C, occasionally exceeding this temperature. Notably, on July 1st , higher temperatures contributed to significant DC power generation, indicating favorable conditions for efficient operation. Despite the increase in temperature, power output rose, with the single-axis subfields achieving more significant gains than the fixed subfields. It suggests that elevated temperatures did not hinder performance but enhanced productivity. On July 1st , conditions were particularly advantageous for both fixed and motorized panels, leading to higher energy yields. A similar trend was observed on May 1st , where rising temperatures also correlated with increased power output. The recorded average temperatures on these days remained within the optimal range for solar panel performance. High temperatures negatively affect the performance of solar panels, as they reduce their efficiency and power output. The evidence for this previous study conducted in Southeast China by Du et al. (2012) [84]

showed that temperatures above 60°C significantly reduce panel power output while lowering the temperature below this threshold increases efficiency and power generation. The panels operated near their optimal capacity since such extreme temperatures were not observed in our experimental study. Since rising temperatures adversely affect the performance of solar panels, finding practical solutions to alleviate this impact is crucial. Researchers such as Mohamed R. Gomaa et al. (2020) [85], Their study experimentally evaluated two cost-effective cooling methods to enhance PV system performance: direct active cooling using water and passive cooling with fins. A non-cooled PV module was used as a reference for comparison. The findings showed that the water cooling method reduced the module surface temperature to 38°C, while the fin cooling method brought it down to 55°C, compared to 58°C for the non-cooled module. These cooling techniques enhanced energy performance, resulting in a 10.2% increase in daily harvested energy for the water-cooled module and a 7% increase for the fin-cooled module. Additionally, the performance ratio improved to 84% with water cooling and 81% with fins, while the non-cooled module had a performance ratio of 77%.

Furthermore, wind speed and humidity significantly impact the efficiency of photovoltaic subfields. During the experimental period, we observed that higher wind speeds and lower humidity levels improved solar panels output. Increased airflow effectively reduced localized humidity on May 1st and July 1st by promoting continuous air movement over the panels. It led to increased power generation. Additionally, motorized subfields outperformed fixed subfields due to the cooling effect of wind, lower atmospheric moisture, and better solar absorption, resulting in consistently superior performance. Our experimental analysis confirmed an inverse relationship between wind speed and relative humidity: as wind speed increased, humidity levels decreased, further supporting these findings. Water condensation on solar panels can decrease their efficiency by causing moisture build-up. To address this issue, we optimize the tilt angle in our subfields , where photovoltaic panels are installed at a fixed tilt of 30°. which allows water droplets to run off rather than accumulate, thus minimizing prolonged moisture exposure. Additionally, natural airflow in well-ventilated areas enhances this effect. On May 1st and July 1st , increased airflow effectively reduced localized humidity by promoting continuous air movement over the panels. This led to higher power gains for the single-axis tracking system and improved overall power generation.

These observations reinforce the idea that a single meteorological factor does not determine a photovoltaic system's ability to convert solar radiation into electrical energy; rather, it is the combined influence of irradiance, temperature, wind speed, humidity, and panel orientation. Under favorable conditions- high irradiance, moderate temperatures, enhanced airflow, and reduced surface moisture - the panels can absorb a greater portion of incoming solar energy, resulting in higher conversion efficiency and improved power output. In particular, single-axis tracking systems show a stronger response to these favorable environmental conditions, as their continuous orientation toward the sun maximizes capture of direct beam radiation while also enhancing natural cooling through increased exposure to wind. This synergistic interaction among optimal tilt alignment, improved heat dissipation, reduced moisture accumulation, and maximum irradiance collection significantly contributes to the superior performance of single-axis tracking subfields compared to fixed systems in desert environments such as OUED-NECHOU.

In regions like OUED-NECHOU, which are generally hot and dry but can occasionally experience localized humidity, additional measures can further optimize PV performance. Installing small fans or passive ventilation systems activated by humidity sensors can help remove water droplets from the panel surface while keeping energy consumption minimal. This approach ensures efficient panel operation without compromising energy production, particularly for single-axis systems designed to capture maximum solar radiation. By combining these environmental insights with practical mitigation strategies, PV systems can maintain higher efficiency and more stable power output under varying desert conditions.

9. Augmentation Percentage

The concept of "Augmentation Percentage" in the realm of renewable energy, particularly photovoltaic technologies, denotes the relative enhancement in the performance of a specific technology or system compared to a reference or baseline technology. This metric is determined by calculating the percentage increase or decrease in a particular performance indicator (e.g., power output or efficiency) of the new or alternative technology relative to the baseline [47].

Baseline Technology: This term refers to the standard or reference photovoltaic (PV) technology or system used as a starting point for comparison. It signifies the most prevalent, widely used, or preferred technology in your study.

The percentage of augmentation would be calculated as follows:

$$AP(\%)=\frac{P_{baseline}-P_{new}}{P_{baseline}}\times 100 \quad (2)$$

AP: Augmentation Percentage (%).
$P_{baseline}$: Mean Output Power (KW) of the baseline (reference) technology or subfield.
P_{new} : Mean Output Power (KW)of the new technology or subfield.

The performance improvement of two single-axis tracking sub-fields was evaluated in comparison to two fixed photovoltaic sub-fields during a four-day experimental period in 2016, with each day representing a different season. Monocrystalline (mc-Si) and polycrystalline (pc-Si) silicon technologies were used. Mean output power was measured for both

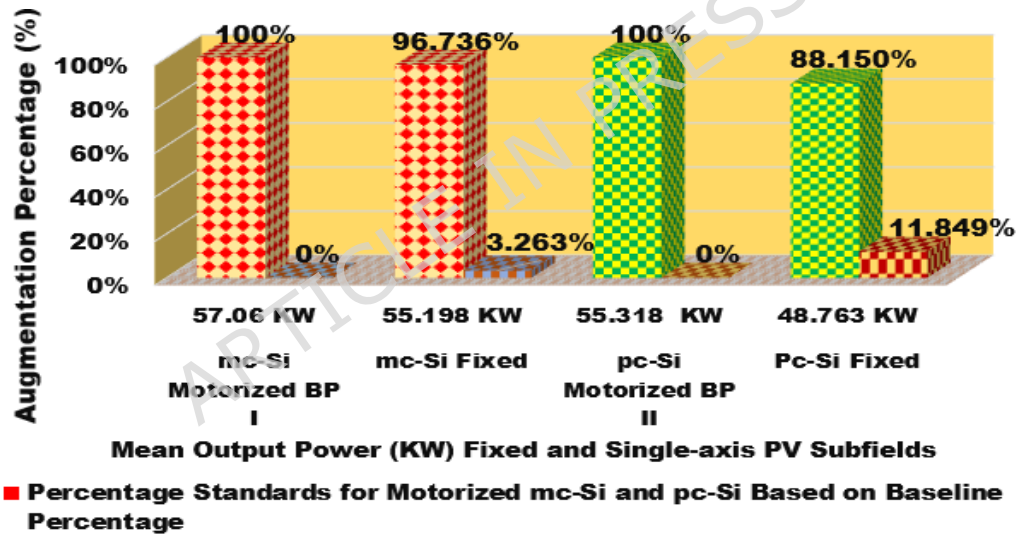

subfield types, and the percentage of augmentation was calculated to quantify the performance gains.

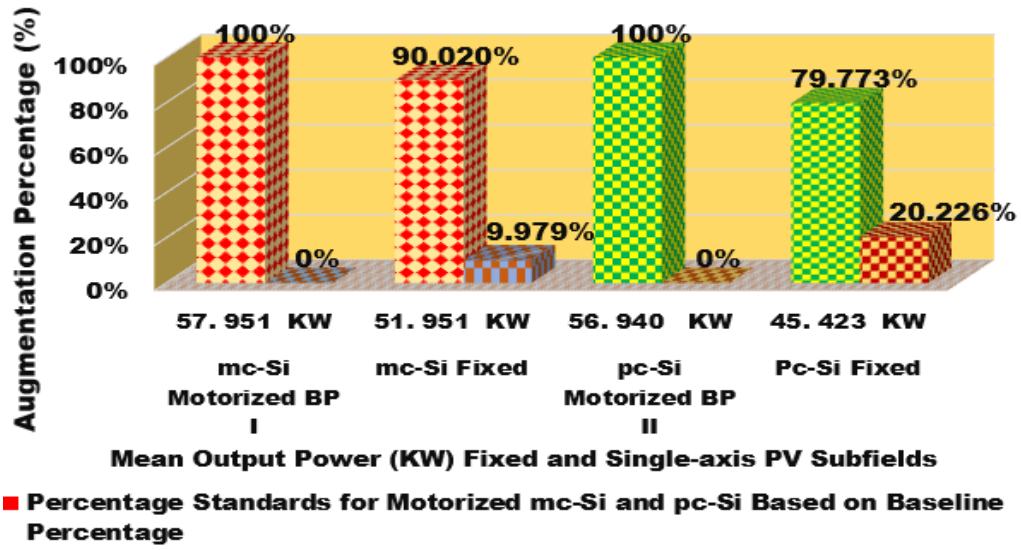

Figure 18. Percentage Increase in Mean Output Power for Fixed and Single-Axis Tracking Subfields (mc-Si, pc-Si) on January 1st , 2016 (Winter Day).

Data from January 1st , 2016, shown in Fig.18. Illustrates the increase in mean output power (in kW) for single-axis tracking systems compared to fixed systems for mc-Si and pc-Si sub-fields. The single-axis tracking sub-fields served as baseline technologies for comparison. The mc-Si single-axis tracking system achieved a mean output power of 57.060 kW, representing a 3.263% increase over the fixed sub-field output of 55.198 kW. Similarly, the pc-Si single-axis tracking system generated 55.318 kW, resulting in an 11.849% increase compared to the fixed sub-field output of 48.763 kW.

Figure 19. Percentage Increase in Mean Output Power for Fixed and Single-Axis Tracking Subfields (mc-Si, pc-Si) on May 1st , 2016 (Spring Day).

In Fig. 19. The results of an experiment conducted on May 1st , 2016 are presented. The experiment aimed to compare the mean output power of fixed and single-axis tracking systems for mc-Si and pc-Si sub-fields during the Spring .The results show that the single-axis tracking subfield, designated as baseline I for mc-Si and baseline II for pc-Si, significantly outperformed the fixed systems. Specifically, the mc-Si single-axis tracking system achieved a mean output power of 57.710 kW, representing a 9.979% increase over the fixed system's output of 51.451 kW. Similarly, the pc-Si single-axis tracking system

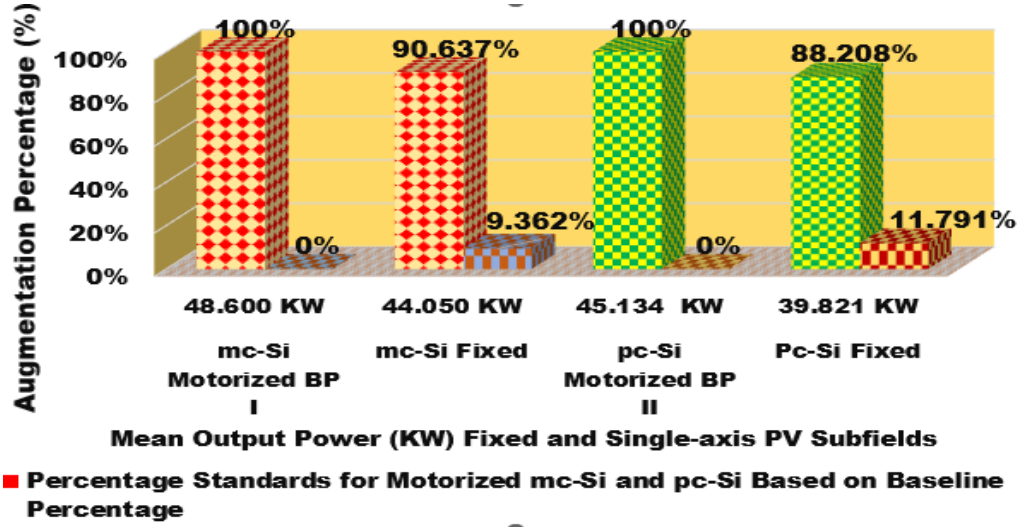

generated 56.940 kW, resulting in a 20.226% increase compared to the fixed system's output of 45.423 kW.

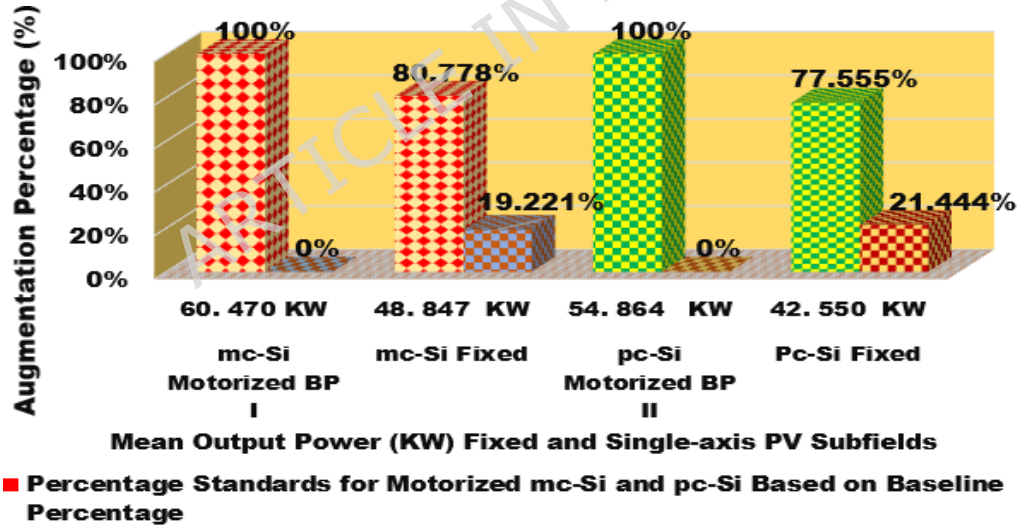

Figure 20. Percentage Increase in Mean Output Power for Fixed and Single-Axis Tracking Subfields (mc-Si, pc-Si) on July 1st , 2016 (Spring Day).

Fig. 20. Presents data on the percentage increase in mean output power (in kW) for single-axis tracking and fixed systems using mc-Si and pc-Si subfields on July 1st , a summer day. The mc-Si single-axis tracking system, considered as Baseline I, achieved a mean output power of 60.470 kW, representing a 19.221% increase over the fixed system's output of 48.847 kW. Similarly, the pc-Si single-axis tracking system, established as Baseline II, generated 54.864 kW, resulting in a 21.444% increase compared to the fixed system's output of 42.550 kW.

Figure 21. Percentage Increase in Mean Output Power for Fixed and Single-Axis Tracking Subfields (mc-Si, pc-Si) on October 1st , 2016 (Spring Day).

On October 1st , on a fall day, Figure 21 depicts the percentage increase in average output power (in kW) for single-axis tracking and fixed systems using mc-Si and pc-Si subfields. The single-axis tracking systems are referred to as Baseline I for the mc-Si sub-field and Baseline II for the pc-Si sub-field. The mc-Si single-axis tracking system achieved a mean output power of 48.600 kW, representing a 9.362% increase over the fixed system's output of 44.050 kW. Similarly, the pc-Si single-axis tracking system generated 45.134 kW, resulting in an 11.791% increase compared to the fixed system's output of 39.812 kW.

The empirical data clearly demonstrates that single-axis tracking systems lead to a substantial increase in the daily average power output (kW) for both mc-Si and pc-Si subfields compared to fixed subfields. This underscores the crucial role of tracking mechanisms in enhancing subfield performance, especially in regions with high solar radiation, diverse sun paths, and favorable weather conditions.

8.1 Experimental Evaluation of Daily Energy Output in PV Subfields

All photovoltaic (PV) subfields have the same power capacity, with a rated instantaneous output of 100 kW. Figure 22 displays the results of a comparative experimental analysis of daily energy production between fixed and single-axis tracking subfields ,conducted over four days, each representing a different season. This study investigates how solar irradiance influences energy variations, emphasizing its role in enhancing productivity in photovoltaic subfields, particularly when utilizing a mechanical tracking system. To ensure accuracy and reliability, energy generation data was recorded at four-minute intervals throughout the daily measurement period.

Figure 22. Comparison of Daily Energy Generation in Fixed and Single-Axis Tracking PV Subfields Across Four Experimental Days .

On January 1st , in winter, the single-axis mc-Si subfield recorded the highest energy output at 547.73 kWh/day, followed by the single-axis pc-Si system, which yielded 531.05 kWh/day. In comparison, the fixed mc-Si system generated 529.92 kWh/day, while the fixed pc-Si subfield produced the least energy at 468.14 kWh/day. The overall low energy production observed on January 1st can be attributed to the weak solar radiation and the shorter duration of daylight typical of winter.

The data recorded on May 1st highlights the seasonal effects on energy production. During the spring season, energy production saw a significant increase due to the transitional seasonal conditions. The mc-Si single-axis system achieved a peak output of 750.24 kWh/day, while the pc-Si single-axis subfield generated 646.85 kWh/day. The fixed mc-Si configuration also performed well, producing 671.50 kWh/day, whereas the fixed pc-Si system generated 590.50 kWh/day.

The highest recorded energy output was observed on July 1st , during the summer season. The mc-Si single-axis subfield achieved its peak generation, producing 787.94 kWh/day, while the pc-Si single-axis system closely followed with 715.17 kWh/day. Among the

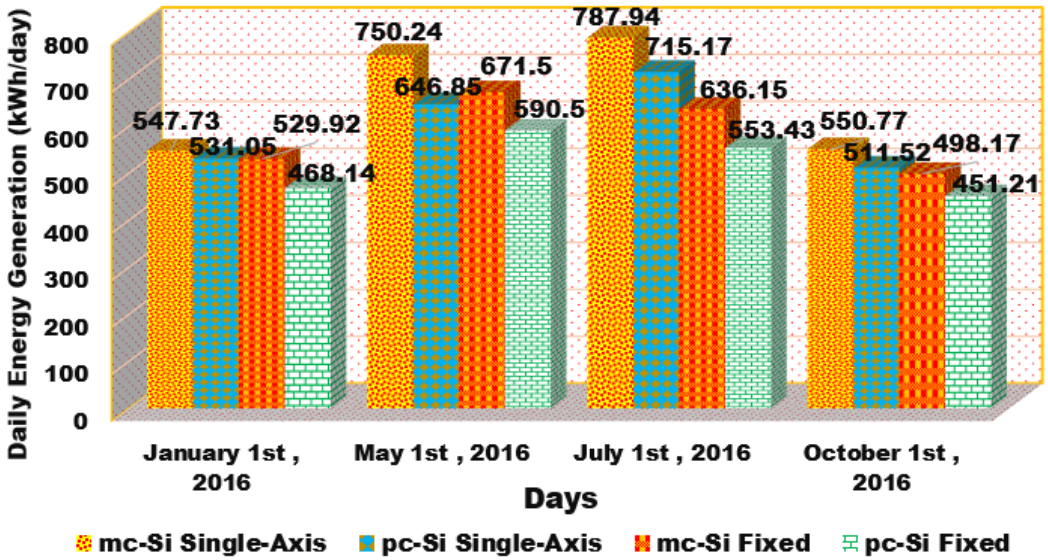

fixed systems, the mc-Si subfield generated 636.15 kWh/day, whereas the pc-Si fixed system recorded the lowest output for this period at 553.43 kWh/day. This notable

increase in performance is attributed to extended daylight hours and higher irradiance levels during the summer.

As fall began on October 1st , a decline in energy generation was observed. The mc-Si single-axis subfield led the performance with an output of 550.77 kWh/day, followed by the pc-Si single-axis system, which generated 511.52 kWh/day. The fixed mc-Si system produced 498.17 kWh/day, while the fixed pc-Si subfield had the lowest recorded energy output for this period, generating only 451.21 kWh/day.

The superior energy yield of motorized subfields is attributed to their ability to continuously track the sun's position throughout the day, maximizing the capture of solar irradiance. This dynamic orientation reduces angle losses and ensures that the photovoltaic (PV) modules receive optimal sunlight exposure, particularly during the early morning and late afternoon when fixed systems tend to exhibit lower efficiency. Additionally, optimizing the mechanical tilt of solar panels enhances direct irradiance absorption, thereby increasing energy generation. These findings highlighted the benefits of single-axis tracking technology, particularly in regions with high solar potential, where seasonal variations can greatly affect photovoltaic efficiency.

9 . Limitations of the study

Despite its valuable contributions to understanding the performance of fixed and single-axis PV systems under real desert conditions, this study has certain limitations. The experimental analysis was limited to four days representing different seasons, providing representative seasonal insights but not capturing long-term year-round variability or extreme meteorological conditions. The results are site-specific to the OUED-NECHOU region in Ghardaïa, characterized by Saharan climatic conditions with high solar irradiance and notable variations in ambient temperature, wind intensity, and humidity; therefore, the findings may not be directly generalizable to regions with different environmental or irradiance profiles. Furthermore, the study focused exclusively on crystalline silicon technologies—monocrystalliene (mc-Si) and polycrystalline (pc-Si)—without considering other photovoltaic technologies, such as thin-film or bifacial modules, which may behave differently under similar conditions. Future research should extend the monitoring period, include additional PV technologies, and integrate economic and degradation analyses to provide a more comprehensive understanding of PV system performance and sustainability. These aspects will be addressed in forthcoming studies to strengthen the findings further.

10. Conclusion

This study systematically compared the performance of four photovoltaic (PV) subfields monocrystalline (mc-Si) and polycrystalline (pc-Si) -in fixed and single-axis tracking (East-West) configurations, each with a 30° tilt and 100 kWp capacity. Performance was analyzed over four days representing different seasons under varying meteorological conditions to determine the most effective configuration.

The semi-empirical PERRIN DE BRICHAMBAUT model was used to forecast solar flux on the 30° inclined surface in real time. Statistical analysis demonstrated high model accuracy, with correlation coefficients (CC) between 0.8273 – 0.9668, RMSE of 4.27–7.72 W/m², MAE of 52.27–65.94 W/m², and MAPE of 1.97–8.87%. The small absolute error across most days confirmed that the model closely predicted actual measurements, indicating it can reliably estimate inclined solar irradiance in OUED-NECHOU and similar Saharan regions even in the absence of a meteorological station.

Daily output power data showed that May 1st recorded the highest peak outputs. The fixed mc-Si system reached 95.57 kW, followed by the mc-Si single-axis system at 88.35 kW , the fixed pc-Si subfield at 84.06 kW, and the pc-Si single-axis system at 83.01 kW. Average daily production revealed peak outputs of 60.47 kW (single-axis mc-Si, July 1st), 55.20 kW (fixed mc-Si, January 1st), and 56.94 kW (single-axis pc-Si, May 1st), with 48.76 kW for the same subfield on January 1st .

The analysis of four days of experimental data revealed a strong correlation between meteorological factors—including solar irradiance, cell and ambient temperatures, wind speed, and relative humidity—and PV power output. Higher irradiance levels directly increased power generation, especially in crystalline silicon modules, which showed strong responsiveness to irradiance variations. For instance, the mc-Si single-axis system reached irradiance peaks of 782.51 W/m² on July 1st and 730 W/m² on May 1st , resulting in corresponding rises in power output. The superior performance of the single-axis system is attributed to its motorized tracking mechanism, which continuously aligns the panels with the sun's east–west movement, ensuring optimal solar capture.

PV performance was also influenced by temperature: efficiency remained high within the optimal range around 25 °C, while excessive heat slightly reduced output voltage. On July 1st , the highest average temperature coincided with the greatest power gain in single-axis systems, confirming that temperature played a favorable role under these conditions. Moreover, higher wind speeds and lower humidity on May 1st and July 1st enhanced power generation by cooling the cells, whereas low wind and high humidity on January 1st and October 1st reduced performance due to cloud cover and water condensation on panel surfaces that limited irradiance absorption.

Tracking systems consistently enhanced photovoltaic performance compared to fixed installations. Both monocrystalline (mc-Si) and polycrystalline (pc-Si) single-axis subfields delivered higher power outputs across all experimental days, with the greatest gains observed on July 1st and May 1st . On these dates, the mc-Si tracker generated 19.22% and 9.98% more power gain than its fixed counterpart, while the pc-Si tracker produced 21.44% and 20.23% more than fixed pc-Si subfield, respectively. The lowest gains occurred on January 1st for mc-Si (3.263%) and on October 1st for pc-Si (11.791%).

The analysis confirmed the superior performance of single-axis tracking systems in energy production. On May 1st , they generated 750.24 kWh/day for mc-Si and 646.85 kWh/day for pc-Si, while on July 1st, the outputs reached 787.94 kWh/day and 715.17 kWh/day, respectively. In contrast, fixed systems produced lower values of 671.50 kWh/day and 590.50 kWh/day on May 1st , and 636.15 kWh/day and 553.43 kWh/day on July 1st . These results highlight the effectiveness of tracking mechanisms in maximizing solar energy capture. Overall, the single-axis polycrystalline subfield exhibited slightly higher power gains than the monocrystalline one, while the mc-Si single-axis configuration showed the best overall efficiency in energy production. Therefore, implementing polycrystalline technology is recommended for the OUED-NECHOU region and similar Saharan environments due to its strong adaptability to local conditions .

11. Future Perspectives

Future improvements should focus on optimizing tilt angles and integrating adaptive control algorithms to enhance energy yield. Regular monitoring of photovoltaic (PV) panels is essential, particularly for single-axis tracking systems in dust-prone regions such as OUED-NECHOU. Beyond these practical enhancements, broader research should explore the development of climate-resilient, intelligent tracking systems suited to harsh desert environments. Kumba et al. (2024) [18] provide a comprehensive review of solar tracking systems, discussing key operational and environmental challenges as well as future research directions, including optimization of mechanical architectures and adaptive control strategies. Likewise, Ponce-Jara et al. (2024) [20] demonstrated that single-axis tracking can substantially increase daily and long-term energy yield, although performance is influenced by local irradiance and climatic conditions.

Consistent with these findings, our experimental results in OUED-NECHOU confirmed that motorized single-axis tracking systems significantly enhance daily power production and energy generation across all seasons. Therefore, future studies should incorporate adaptive intelligent controllers, real-time environmental monitoring, predictive maintenance strategies, and alternative performance indicators to further optimize system efficiency, resilience, and durability under desert climatic conditions.

In addition to performance improvements, future research should evaluate the economic viability of single-axis tracking systems in the regional context. Recent techno-economic analyses Gol & Ščasný., 2023 [86] show that one-axis trackers produce 20–30% more energy than fixed systems and achieve a lower LCOE. Demirdelen et al., 2023 [87] demonstrated that in Mediterranean climates, tracking systems offer significantly faster payback compared to fixed installations. Furthermore, Ayadi et al. (2024) [88] reported that in desert conditions, bifacial 1-axis tracking configurations can achieve a competitive LCOE of as low as ~2.45 ¢/kWh under favorable circumstances. Building on these insights, we plan to conduct a long-term, region-specific techno-economic assessment for OUED-NECHOU, including LCOE modeling, life-cycle costing, and maintenance cost projections. By integrating both performance and economic perspectives, future research will contribute to designing optimized, reliable, and cost-effective PV systems tailored to challenging desert environments like OUED-NECHOU.

Data Availability Statement: The datasets used and/or analyzed during the current study are available from the corresponding author upon reasonable request.

Funding: This work is funded and supported by the Deanship of Graduate Studies and Scientific Research, Taif University

Acknowledgments: The authors would like to acknowledge the Deanship of Graduate Studies and Scientific Research, Taif University for funding this work.

Author Contributions: Bouramdane Abderraouf, Louazene Mohammed Lakhdar, Benmir Abdelkader, Larouci Benyekhlef: Conceptualization, Methodology, Software, Visualization, Investigation, Writing- Original draft preparation. Salah K. Elsayed, Abdulrahman Babqi, Daniel Limenew Meheretie, Walid S. E. Abdellatif: Data curation, Validation, Supervision, Resources, Writing - Review & Editing, Project administration, Funding Acquisition.

Conflicts of Interest: Authors stated that no conflict of Interest.

REFERENCES

[1] Haddad, B., Liazid, A. & Ferreira, P. A multi-criteria approach to rank renewables for the Algerian electricity system. Renewable Energy 107, 462–472 (2017).
[2] Saiah, S. B. D. & Stambouli, A. B. Prospective analysis for a long-term optimal energy mix planning in Algeria: towards high electricity generation security in 2062. Renewable and Sustainable Energy Reviews 73, 26–43 (2017).
[3] Huan, Z., Chuanyu, S. & Mingming, G. Progress in profitable Fe-based flow batteries for broad-scale energy storage. Wiley Interdisciplinary Reviews: Energy and Environment 13 (2024).
[4] Stambouli, A. B., Khiat, Z., Flazi, S. & Kitamura, Y. A review on the renewable energy development in Algeria: current perspective, energy scenario and sustainability issues. Renewable and Sustainable Energy Reviews 16, 4445–4460 (2012).
[5] Sharma, V. & Chandel, S. S. Performance analysis of a 190 kWp grid interactive solar photovoltaic power plant in India. Energy 55, 476–485 (2013).
[6] Dahmoun, M. E. H., Bekkouche, B., Sudhakar, K., Guezgouz, M., Chenafi, A. & Chaouch, A. Performance evaluation and analysis of grid-tied large-scale PV plant in Algeria. Energy for Sustainable Development 61, 181–195 (2021).
[7] Ascencio-Vásquez, J., Osorio-Aravena, J. C., Brecl, K., Muñoz-Cerón, E. & Topič, M. Typical daily profiles, a novel approach for photovoltaics performance assessment: case study on large-scale systems in Chile. Solar Energy 225, 225–374 (2021).
[8] Bentouba, S., Bourouis, M., Zioui, N., Pirashanthan, A. & Velauthapillai, D. Performance assessment of a 20 MW photovoltaic power plant in a hot climate using real data and simulation tools. Energy Reports 7, 7297–7314 (2021).
[9] Kumar, S. B. S. & Sudhakar, K. Performance evaluation of 10 MW grid-connected solar photovoltaic power plant in India. Energy Reports 1, 184–192 (2015).
[10] S. Touili, S., Alami Merrouni, A., El Hassouani, Y. & Amrani, A. I. Performance analysis of large-scale grid-connected PV plants in the MENA region. International Journal of Engineering Research in Africa 42, 139–148 (2019).
[11] Gómez-Uceda, F. J., Ramirez-Faz, J., Varo-Martinez, M. & Fernández-Ahumada, L. M. New omnidirectional sensor based on open-source software and hardware for tracking and backtracking of twin-axis solar trackers in photovoltaic plants. Sensors 21, 1–16 (2021).
[12] Lazaroiu, G. G. C., Longo, M., Roscia, M. & Pagano, M. Comparative analysis of fixed and sun-tracking low-power PV systems considering energy consumption. Energy Conversion and Management 92, 143–148 (2015).

[13] Nsengiyumva, W., Chen, S., Hu, L. & Chen, X. Recent advancements and challenges in solar tracking systems (STS): a review. Renewable and Sustainable Energy Reviews 81, 250–279 (2018).
[14] Wu, C. H., Wang, H. C. & Chang, H. Y. Dual-axis solar tracker with satellite compass and inclinometer for automatic positioning and tracking. Energy for Sustainable Development 66, 308–318 (2022).
[15] Zaghba, L., Khennane, M., Borni, A., Fezzani, A., Hadj Mahammed, I. & Bouchakour, A. Intelligent MPPT control of stationary and dual-axis tracking grid-connected photovoltaic system. Scientific Digital Library 1, 199–205 (2018).
[16] Zaghba, L., Khennane, M., Fezzani, A., Borni, A. & Mahammed, I. H. Experimental outdoor performance evaluation of photovoltaic plant in a Sahara environment (Algerian desert). International Journal of Ambient Energy 43, 314–324 (2019).
[17] Vaziri Rad, M. A., Oopshekan, A., Rahdan, P., Kasaeian, A. & Mahian, O. A comprehensive study of techno-economic and environmental features of different solar tracking systems for residential photovoltaic installations. Renewable and Sustainable Energy Reviews 192, 2020.
[18] Kumba, K., et al., 2024. Solar tracking systems: Advancements, challenges and future directions: A review. Energy Reports, 12, 3566 –3583.
[19] Kumba, K., et al., 2022. Performance Evaluation of a Second-Order Lever Single Axis Solar Tracking System. IEEE Journal of Photovoltaics, 12(5), 1219–1229.
[20] Ponce-Jara, M. A., Pazmino, I., Moreira-Espinoza, Á., Gunsha-Morales, A. & Rus-Casas, C. Assessment of single-axis solar tracking system efficiency in equatorial regions: a case study of Manta, Ecuador. Energies 17(16), 3946 (2024).
[21] Pendem, S. R. & Mikkili, S. Modeling, simulation and performance analysis of solar PV array configurations (series, series–parallel and honey-comb) to extract maximum power under partial shading condition. Energy Reports 4, 274–287 (2018).
[22] Kumar, N. M., Subathra, M. P. & Moses, J. E. On-grid solar photovoltaic system: components, design considerations, and case study. In 4th International Conference on Electrical Energy Systems, Chennai, India, 616–619 (2018).
[23] Bahanni, C., Adar, M., Boulmrharj, S., Khaidar, M. & Mabrouki, M. Analysis of weather impact on the yield of PV plants installed in two antagonistic cities in Morocco. In 5th International Conference on Renewable Energies for Developing Countries, Marrakech, Morocco, 1–6 (2020).
[24] Kawajiri, K., Oozekia, T. & Genchi, Y. Effect of temperature on PV potential in the world. Environmental Science & Technology 45, 9030–9035 (2011).
[25] Bahanni, C., Adar, M., Boulmrharj, S., Khaidar, M. & Mabrouki, M. Performance comparison and impact of weather conditions on different photovoltaic modules in two different cities. Industrial Journal of Electrical Engineering and Computer Science 25, 1275–1286 (2022).
[26] Amelia, A. R., Irwan, Y. M., Leow, W. Z., Irwanto, M., Safwati, I. & Zhafarina, M. Investigation of the effect of temperature on photovoltaic (PV) panel output performance. International Journal of Advanced Science, Engineering and Information Technology 6, 2088–5334 (2016).
[27] Karami, E., Rafi, M., Haibaoui, A., Ridah, A., Hartiti, B. & Thevenin, P. Performance analysis and comparison of different photovoltaic module technologies under different climatic conditions in Casablanca. Journal of Fundamentals of Renewable Energy and Applications 7, 1–6 (2017).
[28] Malvoni, M., Kumar, N. M., Chopra, S. S. & Hatziargyriou, N. Performance and degradation assessment of large-scale grid-connected solar photovoltaic power plant in tropical semi-arid environment of India. Solar Energy 203, 101–113 (2020).
[29] Al-Maghalseh, M. Experimental study to investigate the effect of dust, wind speed and temperature on the PV module performance. Jordan Journal of Mechanical and Industrial Engineering 12, 123–129 (2018).
[30] Kumar, N. M., Gupta, R. P., Mathew, M., Jayakumar, A. & Singh, N. K. Performance, energy loss, and degradation prediction of roof-integrated crystalline solar PV system installed in Northern India. Case Studies in Thermal Engineering 13, 2019.
[31] Correa-Betanzo, C., Calleja, H. & De León-Aldaco, S. Module temperature models assessment of photovoltaic seasonal energy yield. Sustainable Energy Technologies and Assessments 27, 9–16 (2018).
[32] Olukan, T. A. & Emziane, M. A comparative analysis of PV module temperature models. Energy Procedia 62, 694–703 (2014).
[33] Balta, M., Sahin, S., Akgul, S., Kurt, U. & Ozkan, A. Investigation of effects of dust, wind and relative nutrients in solar power plants: Amasya example. Journal of Engineering Research and Applied Sciences 6, 628–633 (2017).
[34] Al-Bashir, A., Al-Dweri, M., Al-Ghandoor, A., Hammad, B. & Al-Kouz, W. Analysis of effects of solar irradiance, cell temperature and wind speed on photovoltaic systems performance. International Journal of Energy Economics and Policy 10, 353–359 (2020).
[35] Ramli, M. A., Prasetyono, E., Wicaksana, R. W., Windarko, N. A., Sedraoui, K. & Al-Turki, Y. A. On the investigation of photovoltaic output power reduction due to dust accumulation and weather conditions. Renewable Energy 99, 836–844 (2016).
[36] Dawoud, M. & Lim, S. C. Performance comparison of fixed and single-axis tracker photovoltaic system in large-scale solar power plants in Malaysia. Industrial Journal of Electrical Engineering and Computer Science 21, 10–17 (2021).
[37] Bentouba, S., Bourouis, M., Zioui, N., Pirashanthan, A. & Velauthapillai, D. Performance assessment of a 20 MW photovoltaic power plant in a hot climate using real data and simulation tools. Energy Reports 7, 7297–7314 (2021).
[38] Lagouch, A., Maouedj, R. & Benatiallah, A. A 5-MWp grid-connected photovoltaic plant's performance analysis and challenges under Algerian Sahara conditions. International Journal of Ambient Energy 45 (2024).
[39] Aoun, N. Energy and exergy analysis of a 20-MW grid-connected PV plant operating under harsh climatic conditions. Clean Energy 8, 281–298 (2024).
[40] Kumar, N. K., Subramaniam, V. & Murugan, E. Performance analysis of large-scale grid-connected PV plants in the MENA Region. Materials Today: Proceedings 5, 1076–1081 (2018).

[41] Singh, R., Kumar, S., Gehlot, A. & Pachauri, R. An imperative role of sun trackers in photovoltaic technology: a review. Renewable and Sustainable Energy Reviews 82, 3263–3278 (2018).
[42] Qader, V., Ali, O. & Hasan, N. An experimental comparison between fixed and single-axis tracking photovoltaic solar panel performance: Zakho City as case study. Al-Rafidain Engineering Journal 28, 272–279 (2023).
[43] Kabir, M. H., Jihad, M. H. A. & Chowdhury, S. Analysis of solar panel power investigation using fixed-axis, single-axis and dual-axis solar tracker. Procedia Computer Science 282, 708–714 (2025).
[44] Rezk, H., Gomaa, M. R. & Mohamed, M. A. Energy performance analysis of on-grid solar photovoltaic system—a practical case study. International Journal of Renewable Energy Research 9 (2019).
[45] Gomaa, M. R., Hammad, W., Al-Dhaifallah, M. & Rezk, H. Performance enhancement of grid-tied PV system through proposed design cooling techniques: an experimental study and comparative analysis. Solar Energy 211, 1110–1127 (2020).
[46] Hashim, S. M. & Hassan, R. I. Impact of high temperature on PV productivity in hot desert climates. Green Technology, Resilience and Sustainability 2 (2022).
[47] https://www.google.com/earth
[48] Kalu, C., Ezenugu, I. A. & Umoren, A. M. Comparative study of performance of three different photovoltaic technologies. Materials and Software Engineering 2, 19–29 (2019).
[49] Allouhi, A., Saadani, R., Kousksou, T., Saidur, R., Jamil, A. & Rahmoune, M. Grid-connected PV systems installed on institutional buildings: technology comparison, energy analysis and economic performance. Energy and Buildings 130, 188–201 (2016).
[50] Al-Otaibi, A., Al-Qattan, A., Fairouz, F. & Al-Mulla, A. Performance evaluation of photovoltaic systems on Kuwaiti schools' rooftop. Energy Conversion and Management 95, 110–119 (2015).
[51] Marion, B. & Smith, B. Photovoltaic system derived data for determining the solar resource and for modeling the performance of other photovoltaic systems. Solar Energy 147, 147–357 (2017).
[52] Gougui, A., Djafour, A., Khelfaoui, N. & Boutelli, H. Empirical models validation to estimate global solar irradiance on a horizontal plane in Ouargla, Algeria. In AIP Conference Proceedings (2018).
[53] Sidibba, S. & Bah, E. Characterization and modeling of solar radiation on the ground, application to the estimate of solar potential available on the coast of Nouakchott. Materials and Devices 4, 1 (2019).
[54] de Brichambaut, C. P. Estimation of energy resources in France. Notebooks of the A.F.E.D.E.S, No. 1 (1975).
[55] Bayrakçı, H. C., Demircan, C. & Keçebaş, A. The development of empirical models for estimating global solar radiation on horizontal surface: a case study. Renewable and Sustainable Energy Reviews 81, 2771–2782 (2018).
[56] Namrata, K., Sharma, S. P. & Seksena, S. B. L. Empirical models for the estimation of global solar radiation with sunshine hours on horizontal surface for Jharkhand (India). Applied Solar Energy 52, 164–172 (2016).
[57] Takilalte, A., Harrouni, S., Yaiche, M. R. & Mora-López, L. New approach to estimate 5-min global solar irradiation data on tilted planes from horizontal measurement. Renewable Energy 145, 2477–2488 (2020).
[58] Moummi, A., Hamani, N., Moummi, N. & Mokhtari, Z. Estimation du rayonnement solaire par deux approches semi-empiriques dans le site de Biskra. In Proceedings of the 8th International Meeting on Energetical Physics, Béchar, Algeria, November 2006.
[59] El Mghouchi, Y., Chham, E., Krikiz, M. S., Aizoul, T. & El Bouardi, A. On the prediction of the daily global solar radiation intensity on south-facing plane surfaces inclined at varying angles. Energy Conversion and Management 120, 397–411 (2016).
[60] Bensaha, A. A., Benkouider, F. & Bekkouche, S. M. A. Estimation du rayonnement solaire en ciel clair par des modèles empiriques: Application au site de Ghardaïa (Algérie). In Proceedings of the 1st International Seminar on the Apport of the Simulation in Technological Innovation, Ghardaïa, Algeria, November 2017.
[61] Hamani, N. Modélisation du flux solaire incident et de la température de sortie dans un capteur solaire à eau avec effet de concentration du rayonnement solaire incident. Doctoral dissertation, Université Mohamed Khider, Biskra, Algeria (2005).
[62] Benbouza, N., Moghalles, M. M. S., El Ayad, A. N. & Amel, B. Optimization of the solar radiation received by photovoltaic panels using solar tracking systems: Study case in south of Algeria. In Proceedings of the 5th International AEGEAN Symposium on Innovation Technologies and Engineering, Izmir, Turkey, February 2022.
[63] Bayrakçı, H. C., Demircan, C. & Keçebaş, A. The development of empirical models for estimating global solar radiation on horizontal surface: A case study. Renew. Sustain. Energy Rev. 81, 2771–2782 (2018).
[64] Boukelia, T. E., Mecibah, M. S. & Meriche, I. E. General models for estimation of the monthly mean daily diffuse solar radiation (Case study: Algeria). Energy Convers. Manage. 81, 211–219 (2014).
[65] Despotovic, M., Nedic, V., Despotovic, D. & Cvetanovic, S. Evaluation of empirical models for predicting monthly mean horizontal diffuse solar radiation. Renew. Sustain. Energy Rev. 56, 246–260 (2016).
[66] Capderou, M. Atlas solaire de l'Algérie. Modèles Théoriques et Expérimentaux, Vol. 1 (Office des Publications Universitaires, Algeria, 1987).
[67] Cubukcu, M. & Gumus, H. Performance analysis of a grid-connected photovoltaic plant in eastern Turkey. Sustainable Energy Technol. Assess. 39, 100724 (2020).
[68] Pirzadi, M. & Ghadimi, A. A. Performance evaluation of first Iranian large-scale photovoltaic power plant. J. Electr. Eng. 51, 19–30 (2020).
[69] Veerendra Kumar, D. J., Deville, L., Ritter III, K. A., Ferdowsi, J. R. F., Gottumukkala, R. & Chambers, T. L. Performance evaluation of 1.1 MW grid-connected solar photovoltaic power plant in Louisiana. Energy 15, 3420 (2020).
[70] Bendaas, I., Bouchouicha, K., Semaoui, S., Razagui, A., Bouchakour, S. & Boulahchiche, S. Performance evaluation of large-scale photovoltaic power plant in Saharan climate of Algeria based on real data. Energy Sustain. Dev. 76, 101293 (2023).
[71] Jamil, I., Lucheng, H., Habib, S., Aurangzeb, M. & Ahmed, E. M. Performance ratio analysis based on energy production for large-scale solar plant. IEEE Access 10, 5715–5735 (2022).

[72] Karami, E., Rafi, M., Ridah, A., Hartiti, B. & Thevenin, P. Analysis of measured and simulated performance data of different PV modules of silicon in Casablanca. In Second International Conference on Smart Applications and Data Analysis for Smart Sites, 27–28 February 2018.
[73] Zaghba, L., Khennane, M., Mekhilef, S., Fezzani, A. & Borni, A. Experimental outdoor performance assessment and energy efficiency of 11.28 kWp grid-tied PV systems with sun tracker installed in Saharan climate: A case study in Ghardaia, Algeria. Sol. Energy 243, 174–192 (2022).
[74] Ameur, A., Sekkat, A., Loudiyi, K. & Aggour, M. Performance evaluation of different photovoltaic technologies in the region of Ifrane, Morocco. Energy for Sustainable Development 52, 96–103 (2019).
[75] Hafez, A. Z., Shazly, J. H. & Eteiba, M. B. Comparative evaluation of optimal energy efficiency designs for solar tracking systems. In Proc. Third International Conference on Advances in Applied Science and Environmental Engineering, 134–141 (2015).
[76] Hussein, L. A., Ayadi, O. & Fathi, M. Performance comparison for sun-tracking mechanism photovoltaic (PV) and concentrated photovoltaic (CPV) solar panels with fixed system PV panels in Jordan. In Proc. 12th International Renewable Engineering Conference, Amman, Jordan, Apr. 2021 (IEEE).
[77] Elkholy, A., Fahmy, F. H., Abou El-Ela, A. A., Nafeh, A. E. S. A. & Spea, S. R. Experimental evaluation of 8 kW grid-connected photovoltaic system in Egypt. J. Electr. Syst. Inf. Technol. 3, 217–229 (2016).
[78] Dabou, R., Bouchafaa, F., Arab, A. H., Bouraiou, A., Draou, M. D., Neçaibia, A. & Mostefaoui, M. Monitoring and performance analysis of grid connected photovoltaic under different climatic conditions in south Algeria. Energy Convers. Manage. 130, 200–206 (2016).
[79] Panagea, I. S., Tsanis, I. K. & Koutroulis, A. G. Climate change impact on photovoltaic energy output: the case of Greece. Clim. Change Future Sustain. 11, 85–106 (2016).
[80] Schwingshackl, C. et al. Wind effect on PV module temperature: Analysis of different techniques for an accurate estimation. Energy Proc. 40, 77–86 (2013).
[81] Kaplani, E. & Kaplanis, S. Thermal modelling and experimental assessment of the dependence of PV module temperature on wind velocity and direction, module orientation and inclination. Sol. Energy 107, 443–460 (2014).
[82] Zainuddin, H., Shaari, S., Omar, A. M., Zain, Z. M., Soumin, J. & Surat, Z. Preliminary investigations on the effect of humidity on the reception of visible solar radiation and the effect of humidity and wind speed on PV module output. AIP Conf. Proc. 2010, 55–58 (2010).
[83] Al-Ghezi, M. K., Ahmed, R. T. & Chaichan, M. T. The influence of temperature and irradiance on performance of the photovoltaic panel in the middle of Iraq. Int. J. Renew. Energy Dev. 11, 501–513 (2022).
[84] Du, B., Hu, E. & Kolhe, M. Performance analysis of water cooled concentrated photovoltaic (CPV) system. Renew. Sustain. Energy Rev. 16, 6732–6736 (2012).
[85] Gomaa, M. R., Hammad, W., Al-Dhaifallah, M. & Rezk, H. Performance enhancement of grid-tied PV system through proposed design cooling techniques: An experimental study and comparative analysis. Solar Energy 211, 1110–1127 (2020).
[86] Gol, A. & Ščasný, M. Techno-economic analysis of fixed versus sun-tracking solar panels. Int. J. Renew. Energy Dev. 12, 615–626 (2023).
[87] Demirdelen, T., Alıcı, H., Esenboğa, B. & Güldürek, M. Performance and economic analysis of designed different solar tracking systems for Mediterranean climate . Energies 16, 4197 (2023).
[88] Ayadi, O., Rinchi, B., Al-Dahidi, S., Abdalla, M. E. B. & Al-Mahmodi, M. Techno-Economic Assessment of Bifacial Photovoltaic Systems under Desert Climatic Conditions. Sustainability 16, 6982 (2024).